ornl

ORNL/TM-11382

OAK RIDGE NATIONAL LABORATORY

MARTIN MARIETTA

Shield Design, Analysis, and Testing Against a 3 km/s Projectile

E. D. Brewer
W. R. Hendrich
D. G. Thomas
J. E. Smith

OPERATED BY
MARTIN MARIETTA ENERGY SYSTEMS, INC.
FOR THE UNITED STATES
DEPARTMENT OF ENERGY

ORNL/TM--11382

DE90 006070

DEFENSE AND SPACE PROGRAMS

Contribution from
Engineering Technology Division

SHIELD DESIGN, ANALYSIS, AND TESTING AGAINST A 3 km/s PROJECTILE

E. D. Brewer
W. R. Hendrich
D. G. Thomas
J. E. Smith

DATE PUBLISHED: JANUARY 1990

Prepared for
U.S. Air Force Weapons Laboratory
Kirtland Air Force Base
Albuquerque, New Mexico
under Interagency Agreement DOE No. 40-1663-AI

Prepared by the
OAK RIDGE NATIONAL LABORATORY
Oak Ridge, Tennessee 37831
operated by
MARTIN MARIETTA ENERGY SYSTEMS, INC.
for the
U.S. DEPARTMENT OF ENERGY
under contract DE-AC05-84OR21400

TABLE OF CONTENTS

LIST OF TABLES

LIST OF FIGURES

ABSTRACT

During the 3-year period of 1987 through 1989, the Advanced Shield Phenomenology Program included a research and development effort, with both experimental and analytical work, to design a low weight, survivable shield against a low hypervelocity kinetic energy weapon threat. The specific projectile used was a 1.75 gram aluminum cylinder, with a length to diameter ratio of one. Impact velocities of 3 km/s and 7 km/s were studied.

Testing was performed at the Arnold Engineering Development Center, Arnold Air Force Base, Tullahoma, Tennessee. Eight shield configurations were tested against the 3 km/s threat specified. One configuration was tested against the same type projectile at 7 km/s. The Hull hydrocode was used for detailed analysis of nineteen impact configurations.

A successful shield was designed for the 3 km/s threat, having a two layer front plate, 15.24 cm of carbon felt disrupters, and a stainless steel back plate. The two layer front plate was composed of a nine-sublayer ceramic cloth plate with an aluminum backup plate. This shield configuration was 41.5% of the areal density (mass per unit area) of the solid aluminum shield required to stop the same (3 km/s) threat. An identical shield configuration was tested at an impact velocity of 7 km/s and was successful again. In comparison with the solid aluminum shield necessary to stop the higher velocity threat, the shield was 16.7% of the areal density.

Due to the limited data obtained, the conclusions reached are primarily indications of promising areas for future work.

1. The 3 km/s threat is potentially quite damaging, especially in comparison with the same projectile at 7 km/s. Weight reduction for a layered shield versus the solid homogeneous aluminum shield is more difficult for the 3 km/s threat than the 7 km/s threat. Successful shields for either impact velocity are not certain to be successful when tested against the different velocity.

2. The front shield is very important in the overall shield performance; wire front shields, the two-layer type front shields, and spaced layer front shields are recommended for further study, for both weight reduction and performance.

3. The analysis of ceramic (brittle) materials should be continued, with an effort devoted to obtaining an accurate hydrocode model for this type of material.

4. Experimental work using ceramic materials should be continued also. Sublayering, confinement, bonding to the backup plate, how the ceramic and projectile interact, and debris/ejecta produced are all areas of interest.

5. In the low hypervelocity region, a transition from ballistics impact phenomena which are dependent upon properties such as strength and hardness, to the hypervelocity impact phenomena which are quite different, is underway. The low hypervelocity region impact phenomena appear to be affected by a range of material properties. Material property effects need to be better defined and characterized.

6. Overall, a significant weight reduction was achieved. Further weight reduction should be obtainable. Additional study of the function and desired characteristics of all the shield layers is recommended.

1. INTRODUCTION

This report covers the research and development efforts performed to design a layered shield to protect against a 3 km/s kinetic energy weapon projectile. Included here are the experimental work and the supporting analyses that combined to produce a shield of low areal density in comparison with the solid aluminum shield required to stop the same threat. The particular threat used in this study was an aluminum cylinder, with a mass of 1.75 grams and a length to diameter ratio of one. Nine tests were performed as part of the development effort. Nineteen analysis configurations were studied.

Testing consisted of firing a cylinder, as described above, into a layered shield configuration. For each test, the projectile line of flight was kept perpendicular to the front shield surface. Front plate configurations were changed, both to optimize shield design for low weight and improved performance and to study the phenomenology of low hypervelocity impact. Experimental procedures, test hardware, and test results are described and discussed fully in the correspondingly entitled report sections.

The hydrocode analysis covered in this report was initiated prior to any testing. A 3 km/s threat was used because of indications from earlier work (Hopkins et al., 1972) that damage produced by a projectile in this velocity range would be at a maximum. Also, there is not a great deal of

research existing for shielding at this velocity, since it falls between velocities in the conventional ballistics area (below 1.5 km/s) and velocities used in work for space-based shielding (above 5 km/s). Velocity effects were studied, using a range from 2.5 to 4.0 km/s. Widely different front plate configurations were analyzed in an attempt to find configurations more likely to succeed when tested. Analysis efforts continued interactively with the experimental work. Study of the dual-front plate configuration was performed after experimental results indicated this type of front plate was very successful.

Also included in this report are comparisons of analytical and experimental results, conclusions reached as a result of this study, and recommendations for further work.

2. EXPERIMENTAL PROCEDURE

Testing was conducted at the Arnold Engineering Development Center, at the Arnold Air Force Base in Tullahoma, Tennessee, using the S-1 Range Light Gas Gun. Several different types of data were recorded, working in coordination with the S-1 Range personnel, including hard and soft flash x-rays and strain gage readings. The detailed test and data acquisition methods are covered fully in a separate report devoted to that subject (Smith, in press) and are thus not included here.

A discussion of the experimental design logic used during testing is included in this report. This experimental design procedure was initiated as part of the Fast Track Shield Program [Oak Ridge National Laboratory (ORNL) staff, 1989] and was further developed during this study. The basic element of this experimental procedure is flexibility during testing. To achieve this flexibility, which in turn allows rapid development of a shield design, a test matrix for design decisions was developed before testing rather than a list of specific configurations to be tested. An example of a matrix used during a test series is shown in Figure 1. Design decisions can be made at any time during a test series allowing use of all known experimental results, especially those of the immediately previous test(s).

Decisions made during testing were based on experimental results that indicated certain performance levels. The criteria for a successful shield were that of a back plate which had bulged or deformed but not perforated in any way, nor had any evidence of spall from the back surface. Shields with either penetration or spallation were classified as failures. In the low velocity testing, no disrupter or back plate configuration changes were made due to the limited number of test shots available. For each test, the front plate configuration was changed. These changes were based primarily on the back plate results of the previous shots. Consideration was also given to the

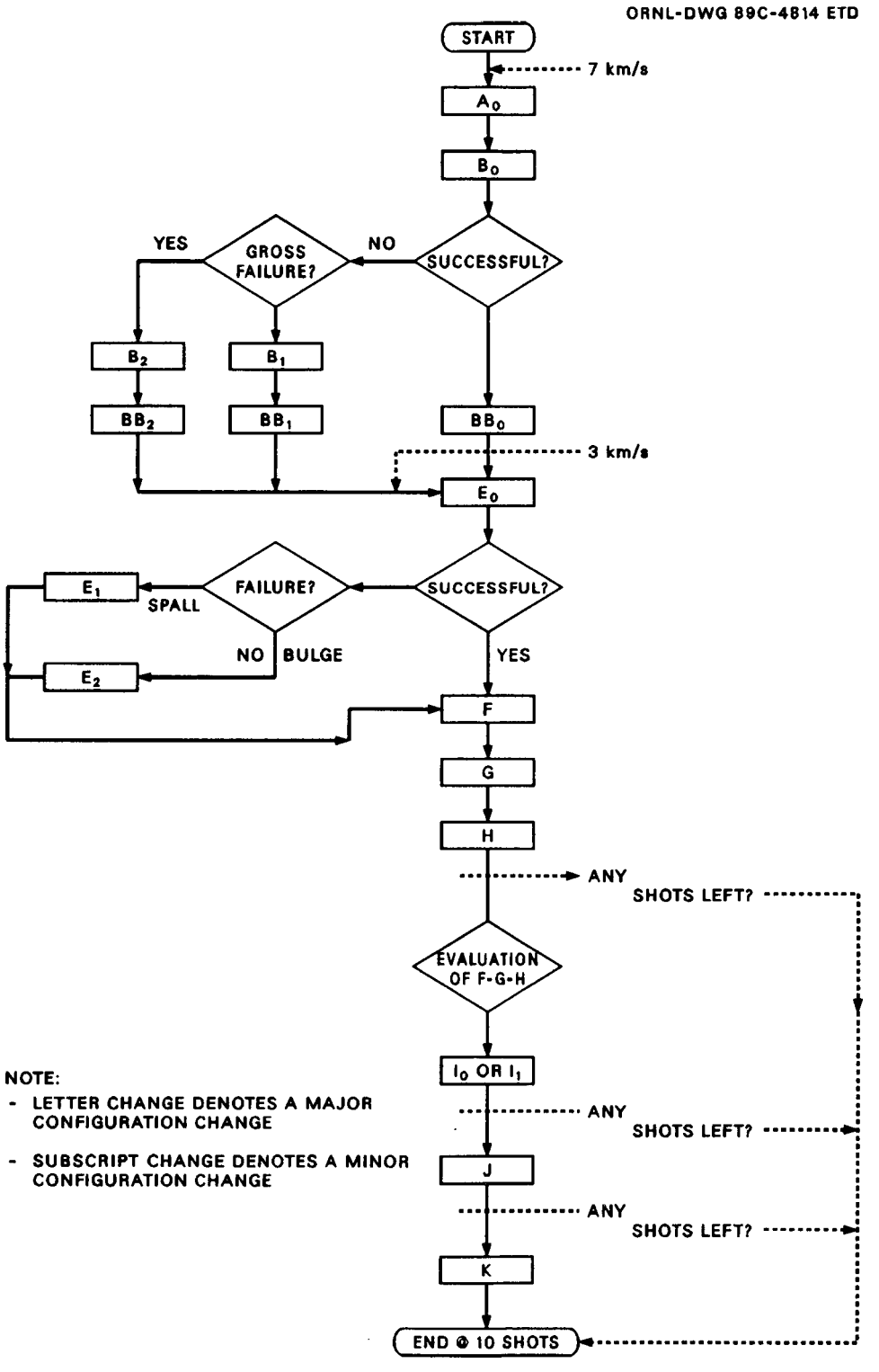

Figure 1. Experimental test design matrix

available results concerning the time from initial impact to the beginning of debris impacts on the back plate. Selection of a 3 km/s shield configuration to be retested at 7 km/s was based on two criteria, a successful performance in the 3 km/s test and low areal density.

Testing against a 3 km/s projectile was performed as part of two test series. In 1988, Series 6 included five tests (68, 69, 71, 72, and 73) at a 3 km/s impact velocity; in 1989, Series 7 included three tests at 3 km/s (78, 79, and 80) and the 7 km/s retest (81) previously mentioned.

3. TEST HARDWARE DESCRIPTION

Eight different shield configurations were tested against a 1.75 gram aluminum projectile at an impact velocity of 3 km/s. One shield configuration was also tested against the same type projectile at an impact velocity of 7 km/s. A solid aluminum shield was tested to provide the baseline reference of bulge without spall for weight reduction comparison. Seven shields were layered configurations, having a front plate, disrupter filling a space, and then a back plate. Six of the seven layered shields incorporated a dual-layer front shield. Figure 2 illustrates the nomenclature used in describing a front shield of this type. All layered stackups used carbon felt, areal density 1.0 gr/cm^2, as the disrupter. The back plate for all seven consisted of 0.069 cm 21-6-9 stainless

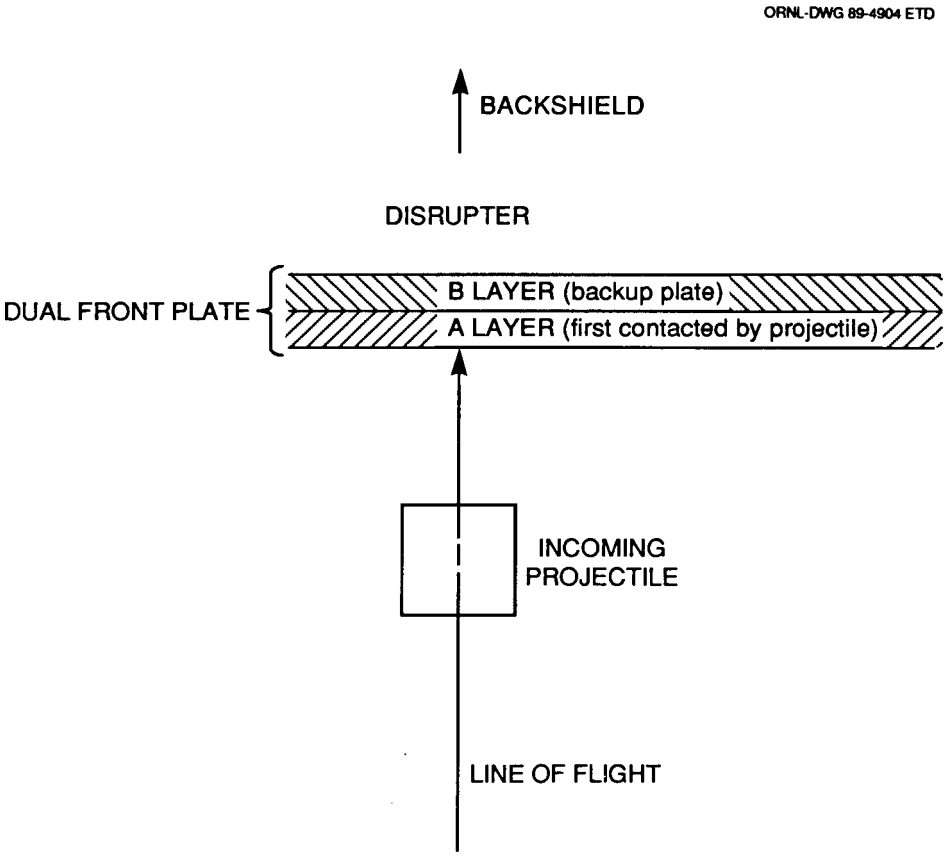

Figure 2. Nomenclature used in a dual front plate configuration

steel. All witness plates were 0.3 cm aluminum, located 2.54 cm behind the back plate. The differences between configurations were all due to different front plates. These are described below in the order tested. In Table 1, a summary of shield hardware is given, along with shield areal densities and comparison with the reference solid shield. For comparison purposes, the solid aluminum reference shield and the lightest weight layered composite shield tested against a 7 km/s aluminum projectile are also included in Table 1.

Shield 68. This is the solid aluminum reference shield necessary to stop the 3 km/s threat. A 3.175 cm thickness of 6061T0 aluminum was used. Areal density of this shield is 8.636 gr/cm^2.

Shield 69. A two-layer front plate was used in this shield. Front plate A was composed of 0.635 cm of K-Karb, a carbon-carbon composite material. Front plate B consisted of 0.635 cm of 1100F aluminum.

Shield 71. For front plate A, 0.614 cm of 85% theoretical density aluminum oxide was used. The B plate was again 0.635 cm of 1100F aluminum.

Shield 72. This shield used an A plate identical to the A plate of Shield 71. Front plate B was essentially the same areal density as the B front plate of Shield 71 but was composed of 0.156 cm of lead rather than aluminum.

Shield 73. The A layer was made up of 4 thin sublayers of a ceramic material, specifically 4 Corelle brand dinner plates. The total thickness of the A layer was 1.016 cm. Again, a 0.635 cm 1100F aluminum B layer was used, as in Shields 69 and 71.

Table 1. Shield hardware summary

Shot no.	Test velocity km/s	Front plate A material	Front plate A thickness cm	Front plate B material	Front plate B thickness cm	Total shield areal density g/cm²	Total shield areal density ratio
68	3	6061T0	3.175			8.636	100.00%
69	3	K-KARB	0.635	AL	0.635	4.234	49.02%
71	3	AL-OX(85)	0.614	AL	0.635	5.388	62.39%
72	3	AL-OX(85)	0.614	LEAD	0.156	5.376	62.25%
73	3	D-WARE	1.016	AL	0.635	5.555	64.32%
78	3	SS WIRES	0.238(dia)			2.525	29.24%
79	3	B-CLOTH	9 layers	AL	0.476	3.584	41.50%
80	3	AL-OX(99)	0.350	AL	0.476	4.197	48.60%
81	7	B-CLOTH	9 layers	AL	0.476	3.574	16.69%
39	7	6061T0	7.870	-	-	21.406	247.87%
41*	7	2024T3	0.160	-	-	2.273	26.32%

Shots 69-81 have 15.24 cm C-FELT disrupter, areal density 1.0 g/cm^2

Shots 69-81 have 0.069 cm 21-6-9 back plate

*15.24 cm C-FELT disrupter, areal density 0.97 g/cm^2; back plate 0.90 cm 304L

Shield 78. The front plate for this shield was quite different, in that the A/B layered configuration was not used. Instead, a front plate of stainless steel wires was used. Each individual wire was 0.238 cm in diameter; wires were located at center-to-center distances of 0.357 cm.

Shield 79. As in Shield 73, the A layer of this shield was multilayered itself. Nine sheets of ceramic cloth (beta-cloth) made up the A layer. For the B layer, 0.476 cm of 1100F aluminum was used.

Shield 80. The A layer was composed of 99.8% theoretical density aluminum oxide, 0.350 cm thick. Small, separate tiles of aluminum oxide were firmly glued using Pliabond to the B layer. The B layer for Shield 80 was the same type as used in Shield 79.

Shield 81. This shield configuration was an exact repeat of shield 79, tested at 7 rather than 3 km/s.

4. TEST RESULTS DESCRIPTION

Table 2 contains a brief summary of the test results. The indication of "success" or "failure" is based on the standard bulge without spall or penetration criteria for the back plate. Also given in Table 2 are times from projectile impact on the front plate to the beginning of debris impact on the back plate. More detailed test results are described in the following report section.

4.1 Front Plate Results

Front plate results for the tests at low velocity were quite different from those seen in the high velocity tests. Referring to other work on high velocity results (ORNL Staff, 1989; Brewer et.al., in press), the front plate damage consisted of small, relatively neat holes in the thin plates used. The low velocity tests produced very different front plate damage, due to the widely different front plates used (both materials and increased thickness) and also to the different velocity. Below, results are briefly described for each test.

Shield 68. The crater produced measured 3.5 cm in diameter and 2 cm deep. On the back surface, the bulge measured 0.35 cm in height.

Shield 69. A large, ragged-edge, almost round hole was produced in the K-Karb plate, varying from 4.6 cm to 4.0 cm in diameter. The average diameter was 4.2 cm. The hole through the aluminum plate was much smaller, from 3.0 to 2.6 cm in diameter with an average diameter of 2.8 cm. Shield 69 is shown in Figure 3.

Shield 71. As shown in Figure 4, the ceramic plate was seriously cracked by the impact. A hole, measuring from 4.0 to 3.6 cm diameter with an average of 3.8 cm, was created. Around the hole is an area of tiny cracks, indicative of brittle failure. Several large cracks extend from the center damage to the edge of the plate. The ceramic plate was held together by the test holder hardware;

Table 2. Test results summary

Shot Number	Back plate description	Witness plate description	Travel time, μ sec	Test Result
68	bulge, 0.35 cm high	-	-	success
69	seven small bulges	-	254	"
71	five small bulges	-	271	"
72	many smaller bulges	-	263	"
73	one large bulge, 1.5 cm high	-	447	"
78	four small buldes, one perforation	perforated	82	failure
79	several small bulges	-	205	success
80	several small bulges, one small split	very minor damage	184	failure
81*	overall bulge, scattered small bulges	-	95 ± 3	success

*repeat of 79 at 7 km/s

ORNL PHOTO 8251-89

Figure 3. Shield 69 front plate damage

at the time for posttest disassembly of the setup, clear tape was used to hold the plate intact for removal. The aluminum B plate hole varied from 2.6 to 2.4 cm in diameter, averaging 2.6 cm.

Shield 72. Front plate damage to the ceramic for shield 72 was almost identical to that for shield 71. The ceramic was less cracked, but the hole produced was the same size and appearance. A significant difference between shield 71 and 72 was the front plate B material and thickness with

ORNL PHOTO 8249-89

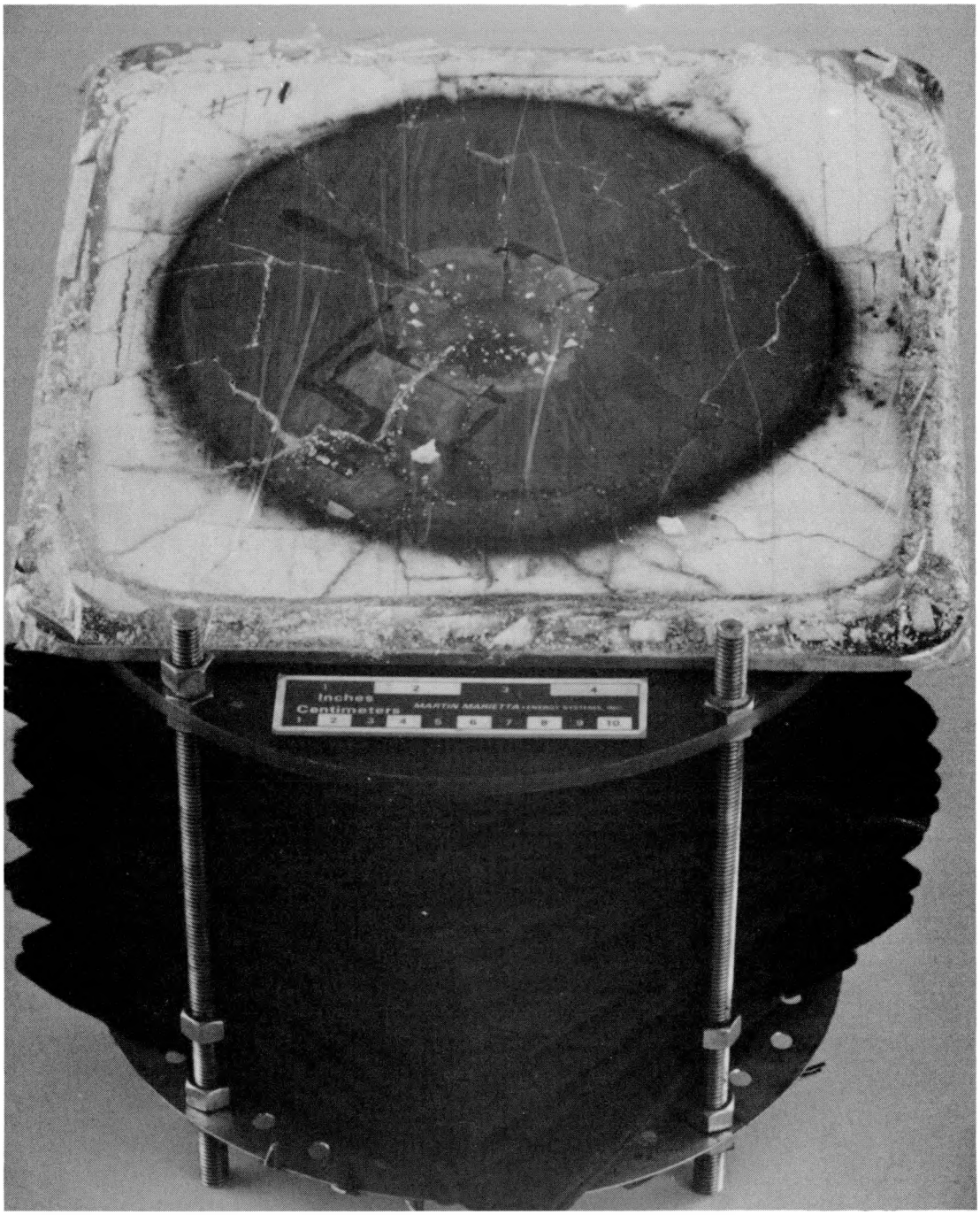

Figure 4. Shield 71 front plate damage

the same areal density. The damage to the B plate of shield 72 was different. As can be seen from Figure 5, the hole in the lead B plate was larger than the hole in the ceramic A plate. In both Figures 3 and 4, the opposite can be seen with the hole in the B plate being visible through the larger hole in the A plate. The hole in the lead measured from 4.4 cm to 4.0 cm and averaged 4.2 cm in diameter.

Shield 73. No hole could be measured for the A front plate, since the ceramic layers were completely shattered into very small pieces. This is shown in Figure 6, which includes some of the debris removed from the test tank. A very nearly circular hole, with average and maximum diameters of 3.6 cm and a minimum of 3.4 cm, was produced in the aluminum B plate.

Shield 78. This shield is shown in Figure 7. Five of the stainless steel wires were broken/damaged by the impact. The resulting hole was elliptical in shape, measuring 2.2 cm on the major axis and 1.5 cm on the minor axis.

Shield 79. Due to the nine layer beta-cloth A plate used, the hole produced was quite ragged, with very many frayed ends of material making a truly accurate measurement of hole diameter almost impossible. A best estimate is approximately 1.5 cm to 2 cm diameter. Figure 8 shows the beta-cloth damage for shield 79. The hole made in the aluminum B plate was slightly larger, measuring 2.5 cm in diameter.

Shield 80. Even though glued to the aluminum B plate, the ceramic tiles used as the shield 80 A plate were broken/shattered/jarred loose by the impact. Figure 9 includes debris removed from the test tank after shield 80. The hole made in the aluminum plate averages 2.3 cm in diameter, with a maximum of 2.4 cm and a minimum of 2.2 cm.

Shield 81. This was an exact repeat of shield 79 but at a test velocity of 7 km/s. The front plate damage to the beta cloth can be seen in Figure 10. Again, exact measurement of the hole diameter is made difficult by the numerous frayed material ends, but a best estimate is

ORNL PHOTO 8248-89

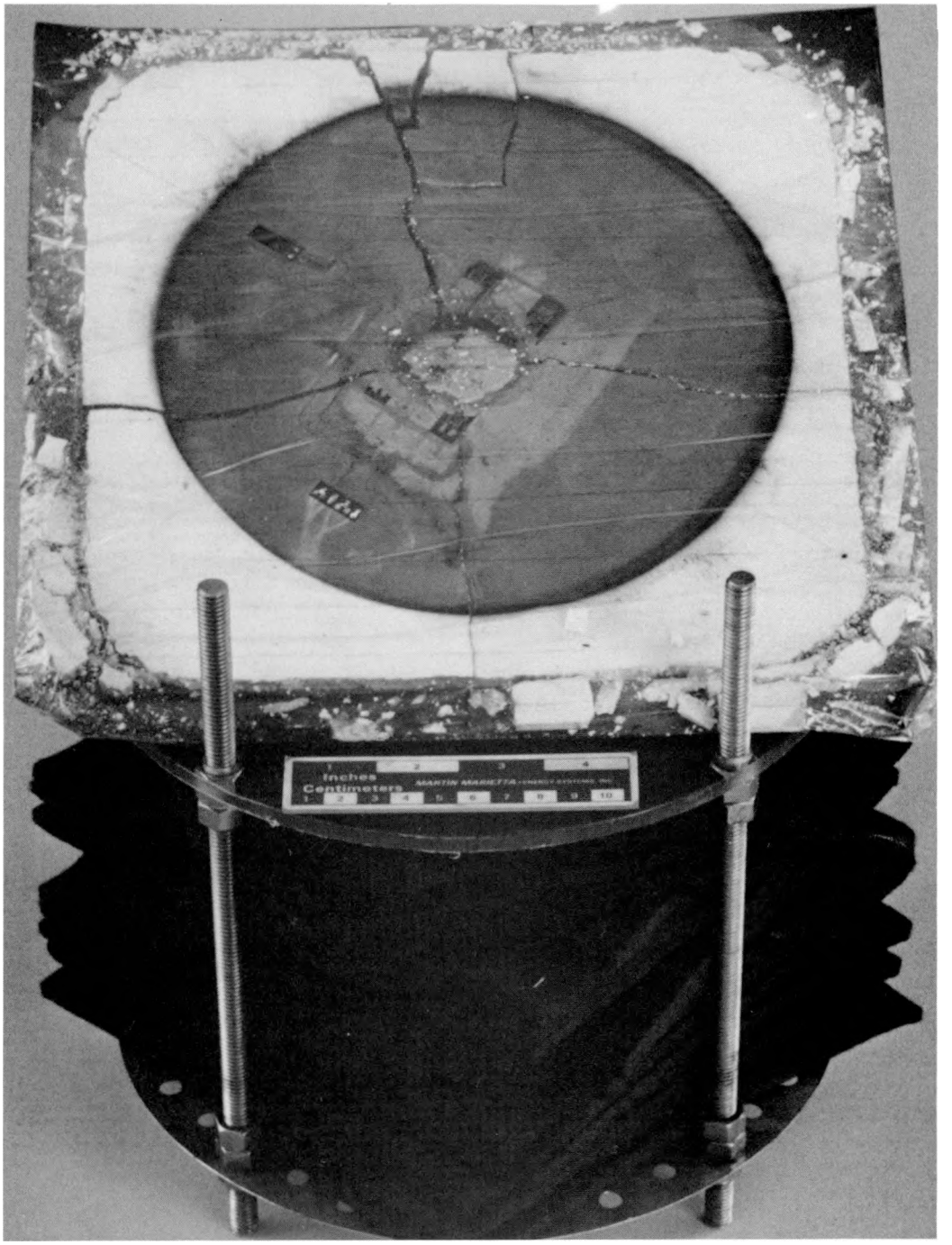

Figure 5. Shield 72 front plate damage

ORNL PHOTO 8250-89

Figure 6. Shield 73 front plate damage

ORNL PHOTO 8242-89

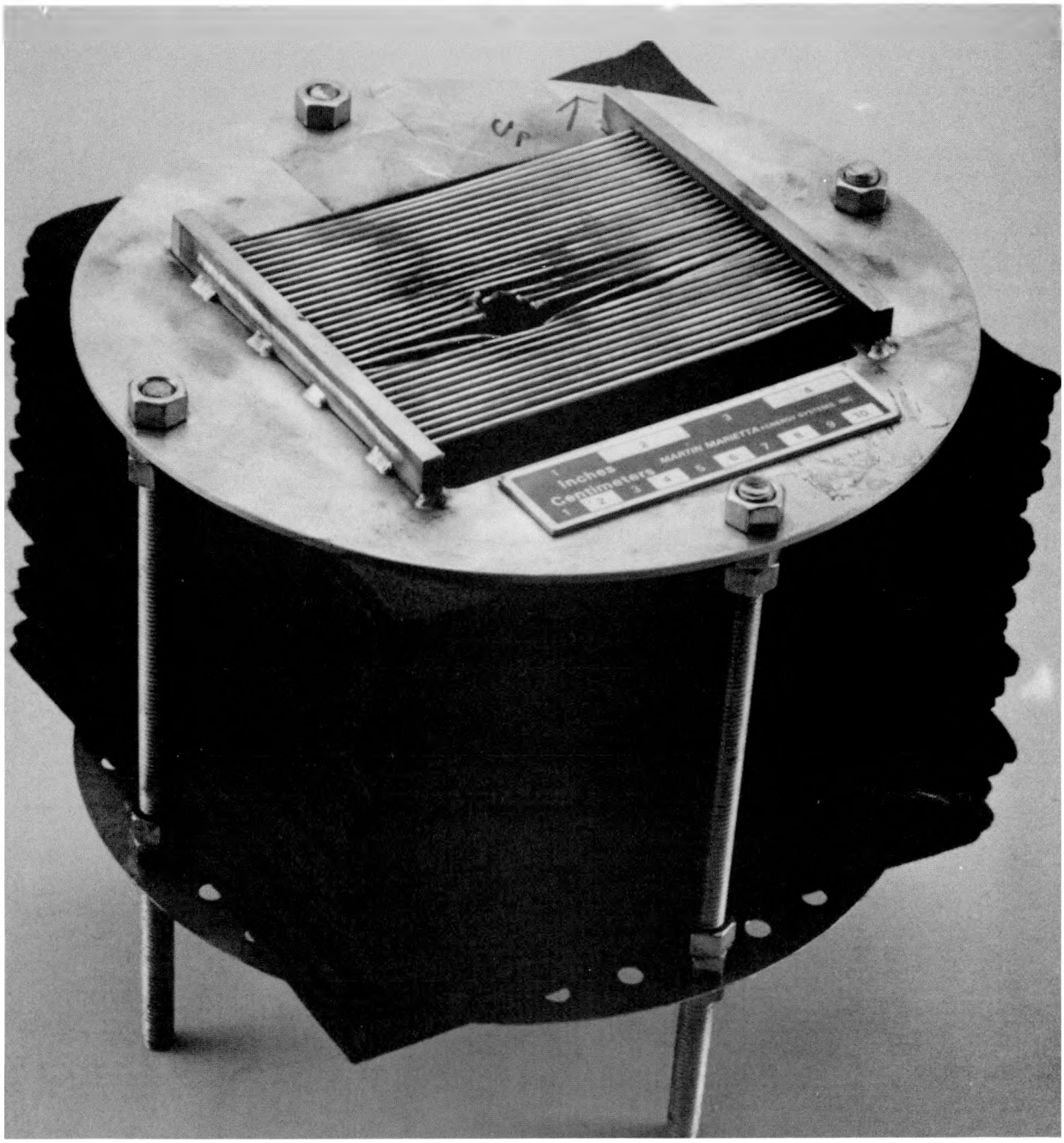

Figure 7. Shield 78 front plate damage

ORNL PHOTO 8244-89

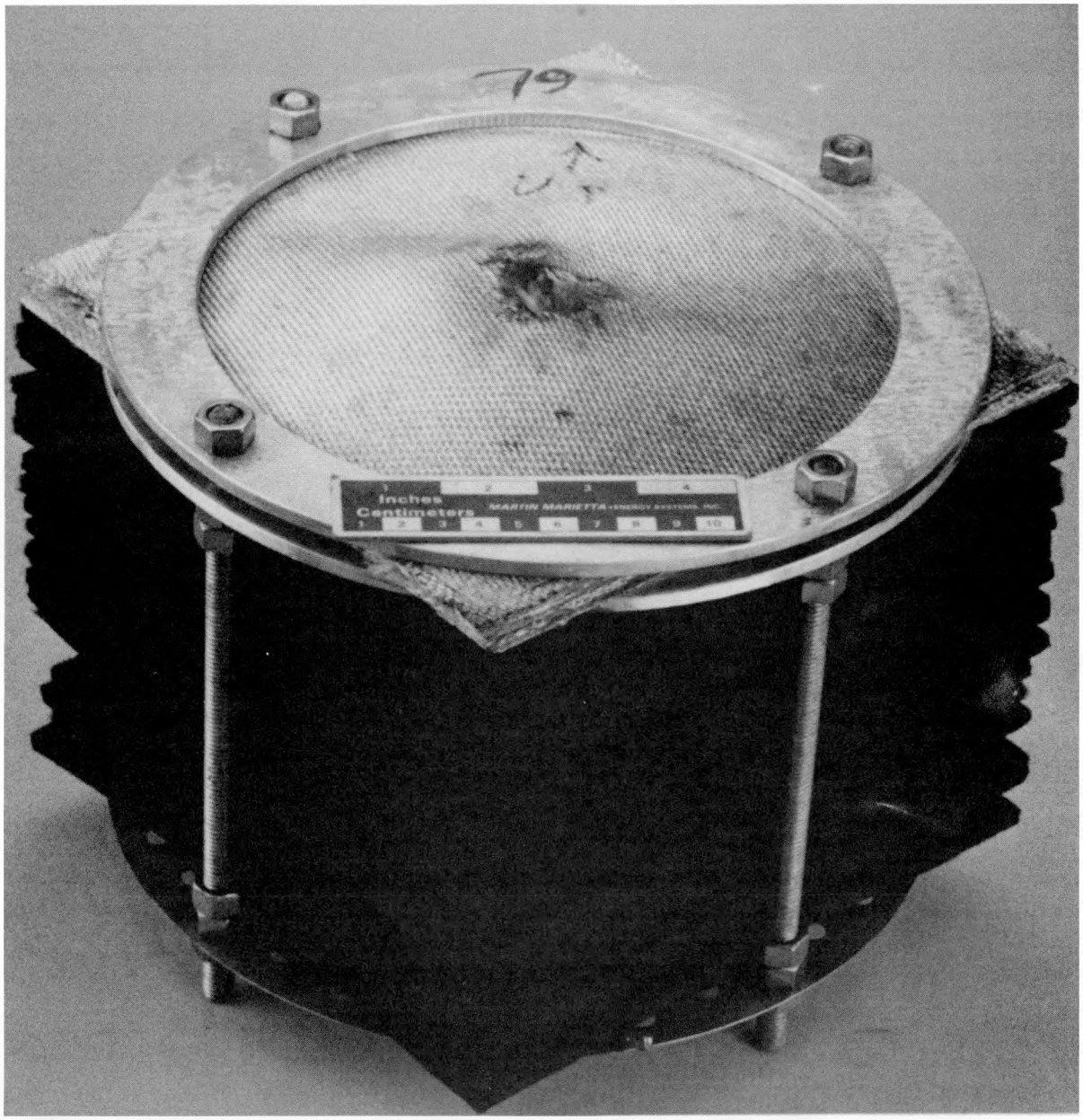

Figure 8. Shield 79 front plate damage

ORNL PHOTO 8243-89

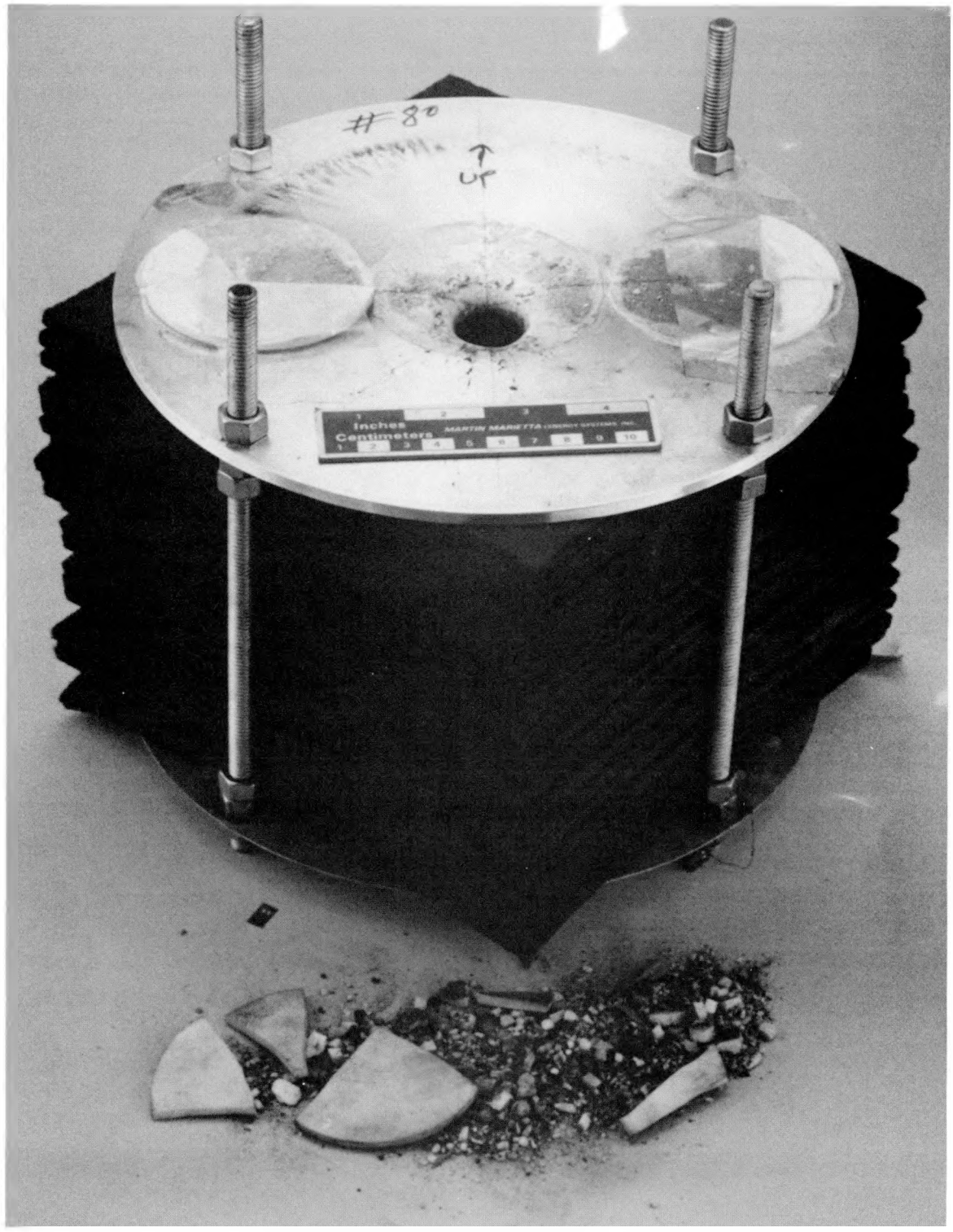

Figure 9. Shield 80 front plate damage

ORNL PHOTO 8245-89

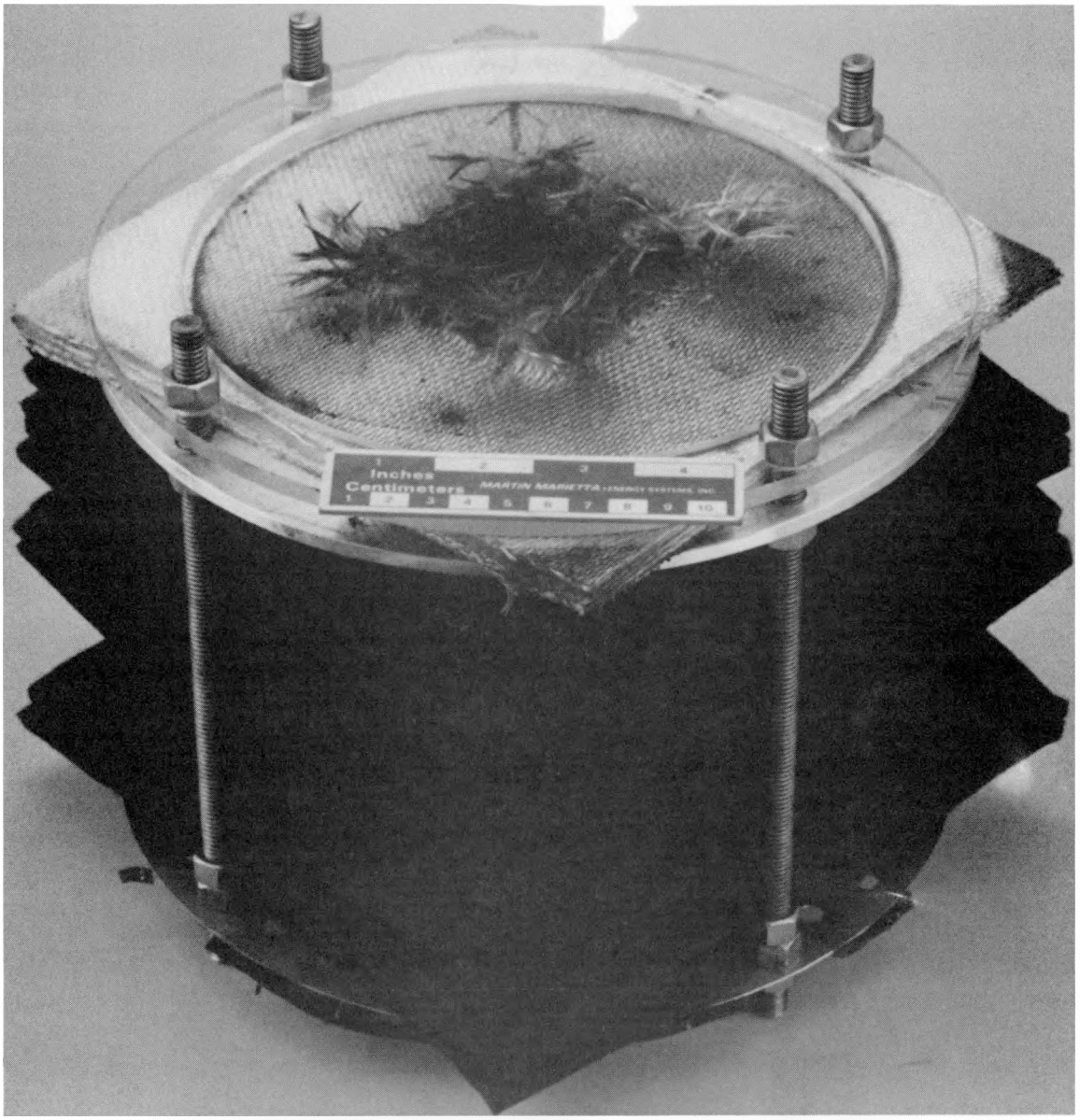

Figure 10. Shield 81 front plate damage

approximately 4.5 cm diameter. The hole in the aluminum B plate measured from 3.6 cm to 3.2 cm in diameter with an average of 3.4 cm. Figure 11 shows shield 79 and shield 81 together for quick comparison.

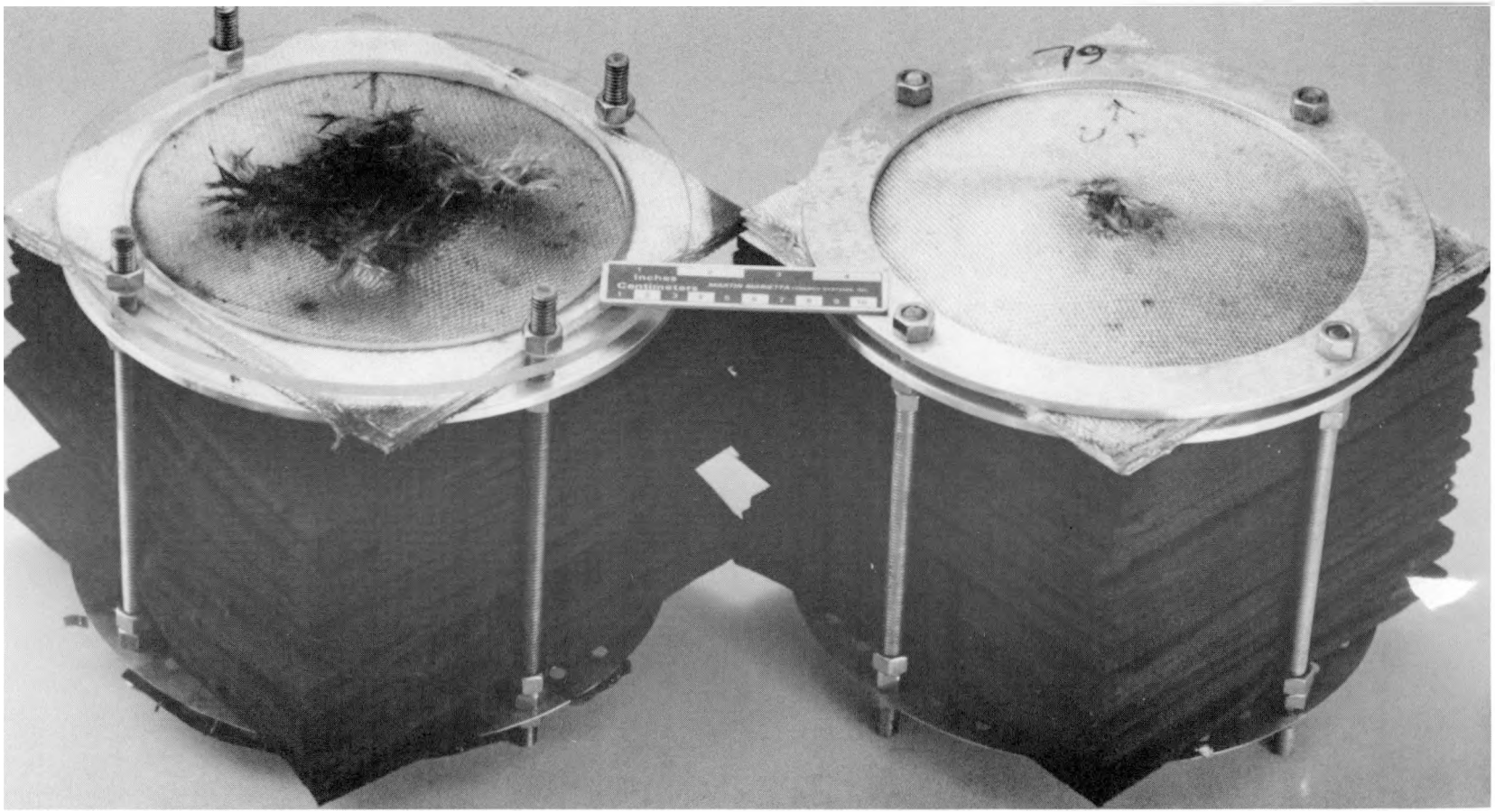

Figure 11. Comparison of shield 79 and shield 81 front plates

4.2 Disrupter Results

Each shield assembly was taken completely apart, and measurements were made of the damage profile in the disrupter layers. The blast damage profiles for each shield are shown in Figure 12. Several notes of interest concerning material found in the disrupter layers are:

1. Shield 69 contained several semi-flat pieces of aluminum, all having the appearance of spall from the back of the B plate, with the largest piece approximately 1 cm in diameter.
2. Shield 71 contained very similar aluminum particles, although none were as large.
3. Shield 72 contained numerous small flat pieces, less than 0.5 cm diameter, of lead imbedded in the disrupter layers. These were found in a "ring" of damage occurring just outside of the main blast damage hole. This is shown in Figure 12, in the plot for shield 72, by the small dots marked on the plot. The "ring" of damage dissolved into or was obliterated by the general blast damage at a depth of 10 cm to 11 cm into the disrupter. Also of interest for shield 72 were the numerous very tiny flecks of ceramic, slightly larger than coarse sand, found sprinkled throughout the disrupter.
4. In shield 73, all disrupter damage was caused by one large semi-flat piece of spall from the back of plate B. The damage profile shown in Figure 12 shows the path of this spall straight from the back of the front plate to the back plate where it was found. The maximum and minimum hole diameters measured in the disrupter layers corresponded to the irregular diameter of the piece of spall. Blast damage outside the hole was due only to tears in the felt at the corners of the hole. The spall piece measured approximately 4 cm in diameter. The weight of the piece after removal of ceramic and carbon dust was found to be slightly over 4 grams.

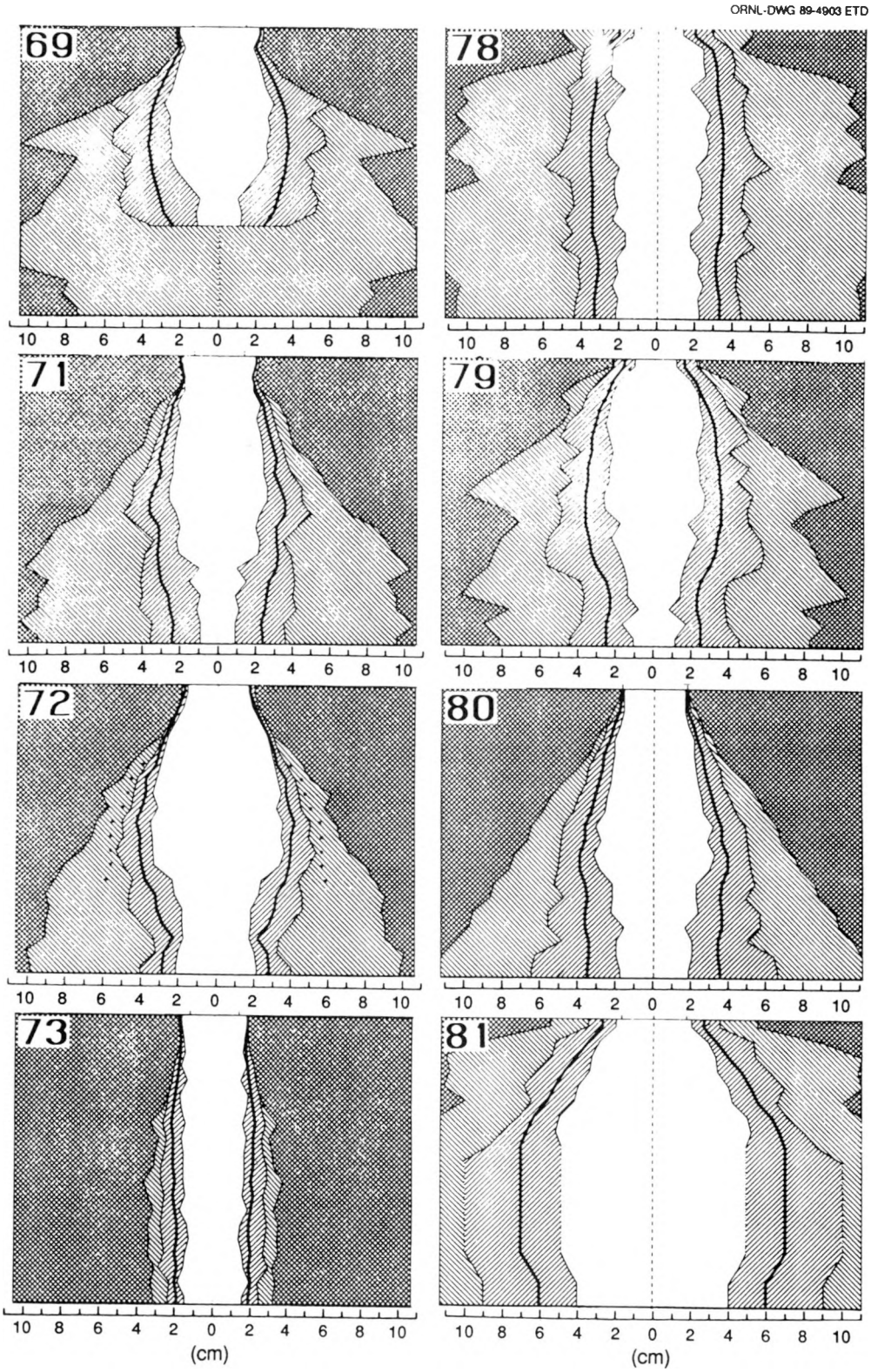

Figure 12. Disrupter damage profiles

5. Shield 79 contained only a few small, less than 0.3 cm diameter, irregularly shaped pieces of aluminum. These did not look like spall; they were all observed to be rough on all surfaces and looked like debris from the edge of the hole in the B plate.
6. Shield 80 contained small aluminum particles similar to those found in shield 79 and those found in shield 71; that is, of the debris found, some appeared to be spall and some appeared to be debris from around the hole edge. There were not as many pieces found for either 79 and 80 as were found for shields 69 and 71.
7. The disrupter for shield 81, as can be seen from the damage profile in Figure 12, was very heavily damaged. Close inspection of Figures 10 and 11 shows the fact that large sections of the disrupter are missing. These were scattered out of the setup by the blast and were recovered from the test tank.

4.3 Back Plate Results

As seen with the front plate damage, back plate damage for the low velocity shields was different than for that seen in the high velocity testing. However, the back plates used were the same, so differences are due to the different velocity and the different front plates rather than the back plates themselves. Results for each back plate, and where applicable, the witness plate, are described below in the order tested.

Shield 69. Only a very slight overall bulge was produced, with numerous small bulges. No breach occurred, as can be seen in Figure 13, which shows the back plates for shields 69, 71, 72, and 73.

Shield 71. The back plate for shield 71 is very similar to that of shield 69, with slightly fewer of the small bulges as the only difference. This is visible in Figure 13.

Shield 72. This plate is very similar from the back side to the plates of shield 69 and 71, in that a very slight overall bulge with small bulges superimposed was produced, and no breach occurred.

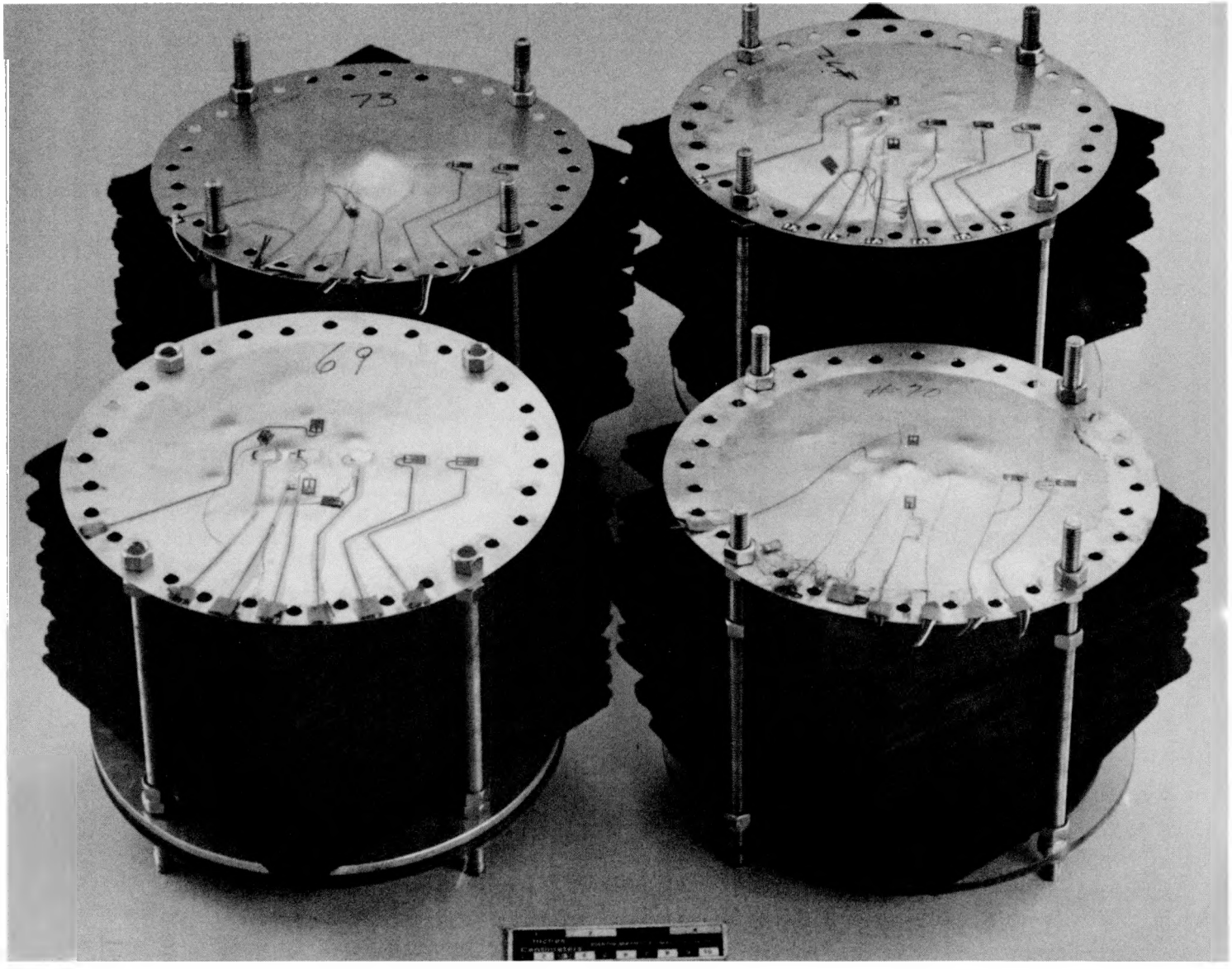

Figure 13. Back plate damage for shields 69, 71, 72, and 73

However, the small bulges are significantly more numerous and smaller in size, as shown in Figure 13. Another difference, which is not apparent from external comparison of the back plates, is found on the inside surface of the back plates. For shields 69 and 71, the inside surface of the shield is smooth like the back surface. On the back, the damage is smooth bulges; on the inside, the damage is smooth craters. This is in contrast to shield 72, which has particles of ceramic embedded in the surface. For each smooth bulge on the back surface, the corresponding inside surface crater has a tiny particle of ceramic embedded in it. These particles can be examined by touch more easily than they can be seen. They feel like a piece of grit.

Shield 73. The back plate of shield 73 has one large bulge superimposed on an almost negligible overall bulge. As indicated from the disrupter results, this was due to the impact of the single large piece of spall debris. The piece of spall is roughly circular but has three tears in it, giving it an irregular, three-lobed appearance. On the back plate, the bulge produced is correspondingly irregularly shaped, and the piece of spall can only be fitted into the bulge in one orientation for a matching fit. Figure 13 also includes the back plate of shield 73.

Shield 78. The back plate of shield 78 was breached in one location. There were also several small bulges produced. Figure 14 shows the back plate for shield 78. The witness plate for shield 78 sustained serious damage and was also perforated.

Shield 79. The back plate damage produced by this shot was very similar to the damage for shields 69 and 71, consisting of a slight overall bulge with several smaller bulges. This is shown in Figure 15.

Shield 80. This back plate is shown in Figure 16. As can be seen in this photograph, the back plate has a slight overall bulge with several smaller bulges. One of the smaller bulges split, resulting in a three-cornered tear. The hole did not petal. The witness plate was almost undamaged.

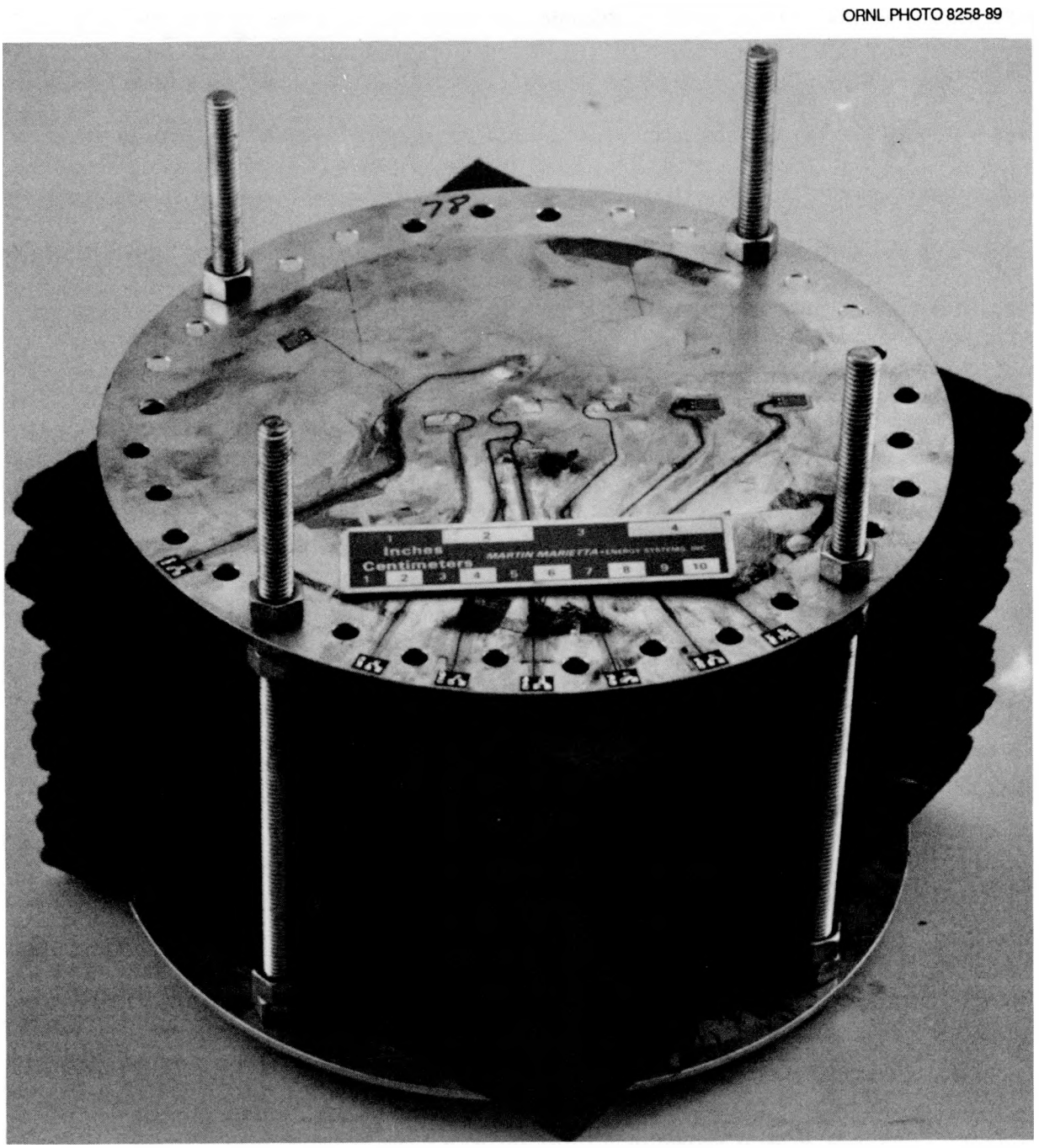

Figure 14. Shield 78 back plate damage

ORNL PHOTO 8247-89

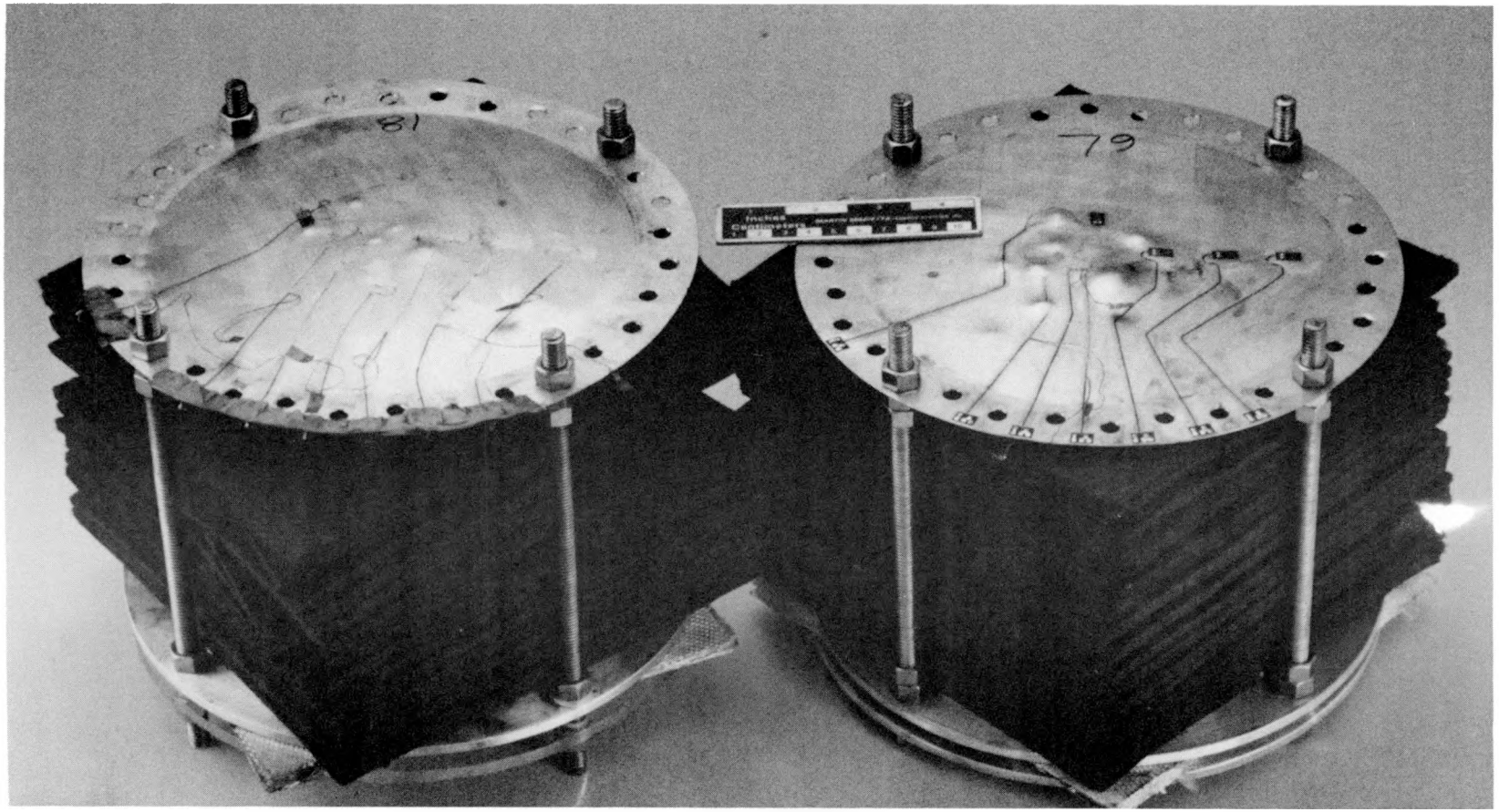

Figure 15. Back plate damage for shields 79 and 81

ORNL PHOTO 8259-89

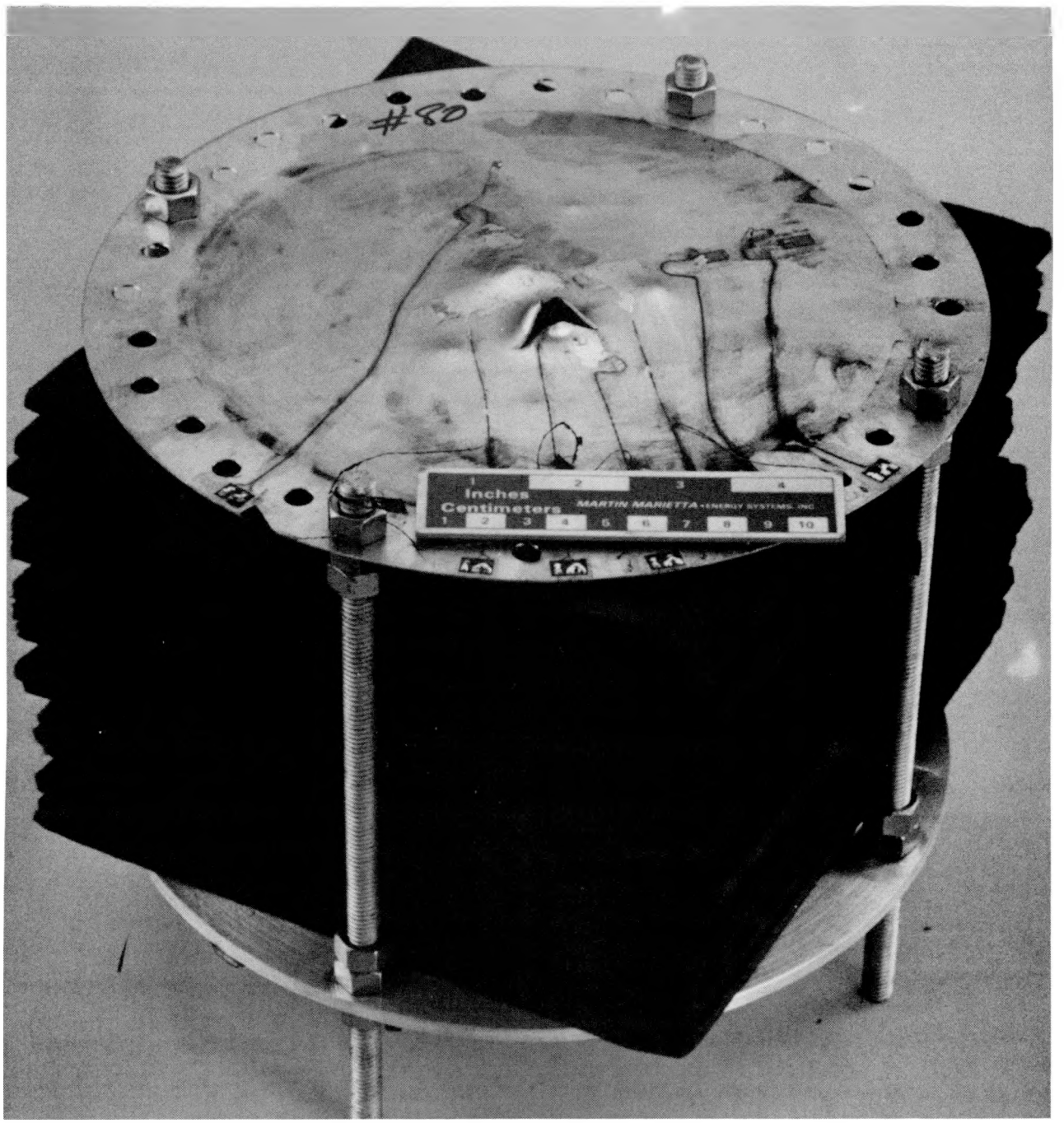

Figure 16. Shield 80 back plate damage

Shield 81. This back plate is also shown in Figure 15. As a repeat of shield 79 at higher velocity, the two are compared. The overall bulge of shield 81 is more pronounced, there were still several small bulges produced, and the small bulges tended to be smaller for shield 81 than shield 79.

5. TEST RESULTS DISCUSSION

Test configurations and results for the 3 km/s study were, as mentioned previously, quite different from the 7 km/s work. An indication of the reason behind this phenomena can be seen in Figure 17, a graph of back shield thickness versus projectile velocity (Hopkins, et. al., 1972). These results are for layered shields. Figure 17 shows a very high damage peak near the 3 km/s velocity with a low damage area occurring in the 7 km/s region. The breakup of the projectile and the state of the projectile debris cause the different damage levels shown in Figure 17, as indicated on the graph. The low hypervelocity region was therefore expected to be quite damaging, and the layered shields tested were configured accordingly.

Shield 68, a solid aluminum shield, was used to obtain a reference for weight reduction using the "bulge without spall or penetration" criteria. The thickness for this shield was calculated correctly for the first test attempt based on the known kinetic energy of the projectile. With the projectile

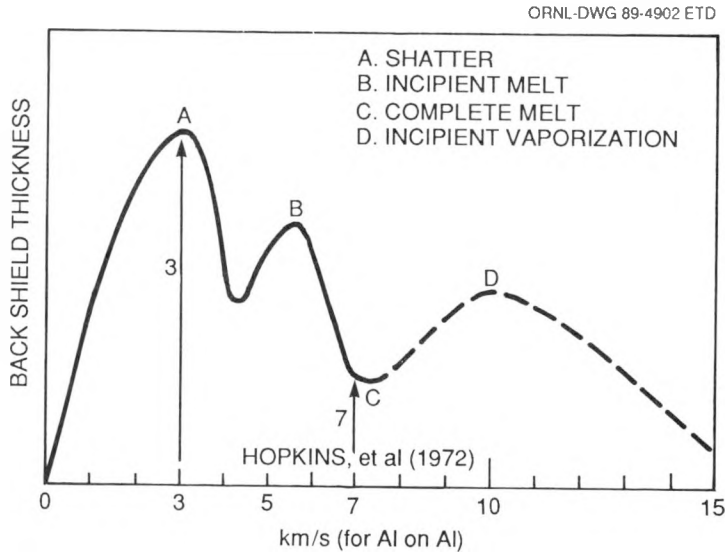

Figure 17. Back plate damage versus velocity

energy as the governing factor in the solid aluminum shield thickness, the 3 km/s reference shield is much thinner than the 7 km/s reference shield. This is shown in Figure 18, which contains both the 3 and 7 km/s reference shields. Comparing the two, the 3 km/s reference shield is 3.175 cm thick (areal density = 8.636 g/cm^2) while the 7 km/s reference shield is 7.870 cm thick (areal density = 21.406 g/cm^2). The 3 km/s shield is 40.3% of the weight for the 7 km/s shield. (As a side note of interest, this comparison is limited to the impact of aluminum projectiles onto aluminum shields. Factors other than projectile energy must be considered for solid shields and projectiles of different materials.)

The two phenomena discussed above, (1) the high damage at 3 km/s for layered shields due to a lack of good projectile breakup and (2) the lower weight of the solid aluminum reference shield for weight reduction measurement, combine to make the shielding problem for the 3 km/s velocity very difficult. Weight reduction is made more difficult by the projectile breakup mode, which inherently limits the effectiveness of the layered shield concept. However, projectile energy rather than projectile breakup is the governing factor for solid shields, and this leads to a lower reference shield for comparison. Thus the problem of low-weight shielding against a 3 km/s threat is doubly difficult when compared to the 7 km/s shielding problem.

The 3 km/s velocity lies above the ballistics range but below the low earth orbit velocity range. In the low velocities of the ballistics range, material properties such as hardness and strength are very important. In the hypervelocity region, materials behave quite differently upon impact, and thus different properties are more important, e.g., the material density, liquification and vaporization change of state energies, etc. Therefore, at the 3 km/s velocity, a transition is underway with different material properties becoming more important. This transition occurs at different rates for

ORNL PHOTO 8252-89

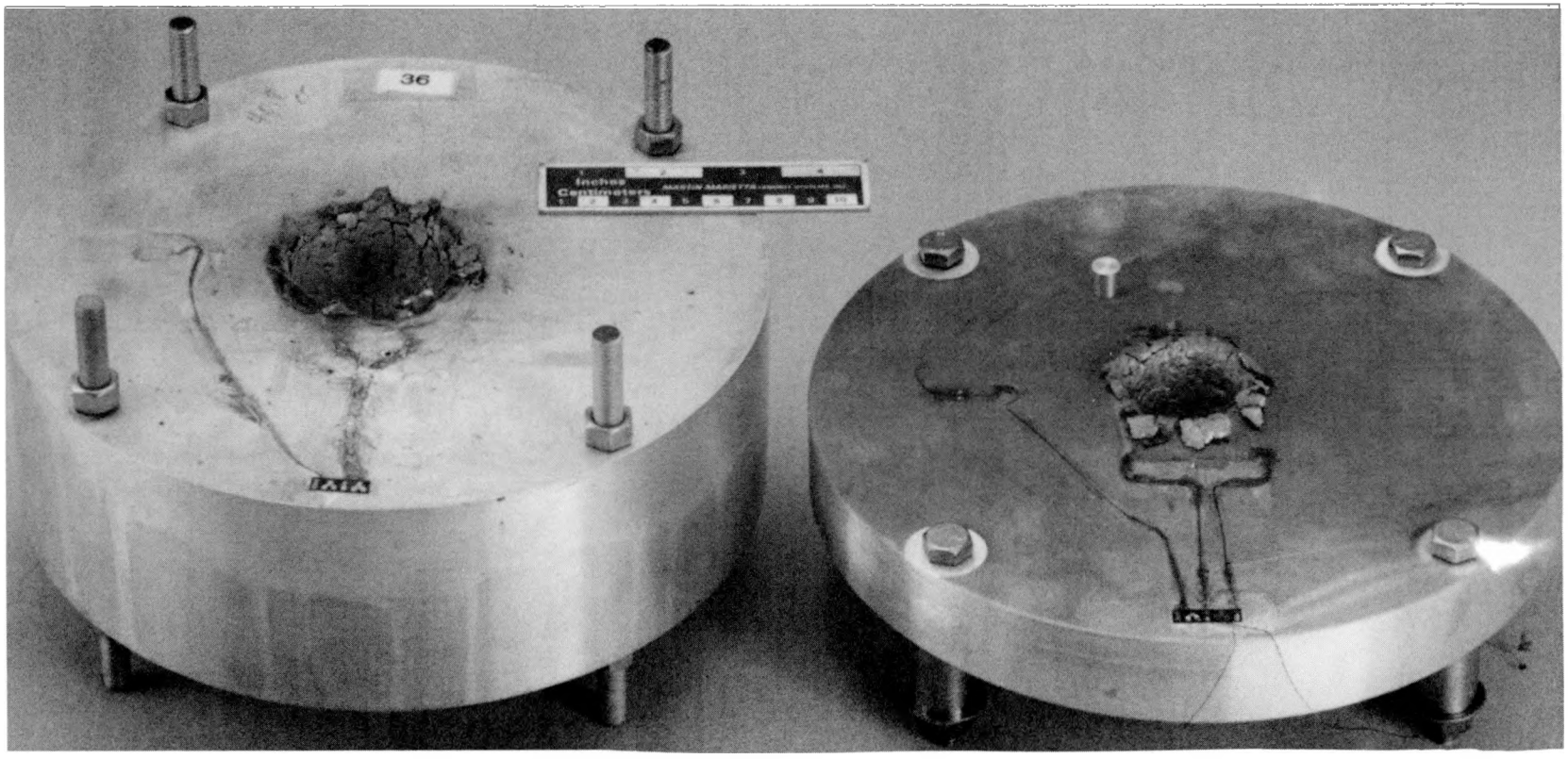

Figure 18. Reference thickness solid shields for 3 and 7 km/s

different materials, and thus itself is dependent on some material property(ies). Thus the selection of materials for the different shield layers is a complex question.

As shown in Figure 17, the same section of the damage curve covers the ballistics region and the velocities around 3 km/s. Therefore, the ballistics area of shielding was researched as a possible starting point (Thomson, 1955; Wilkins et al., 1969; Goldsmith and Finnegan, 1971; Nicol et al., 1988). Referring again to Figure 17 and the appropriate section of the damage curve, the slope of this section is quite steep, indicating a rapid rate of increasing damage with the peak occurring shortly after 3 km/s. Thus the damage at 3 km/s would be much greater than at ballistics velocities and, with the materials properties transition previously mentioned to be considered also, the layered shield designs initially selected for testing were not merely heavy ballistics armor. Using ballistics-type armor, while it might lead to a successful shield in terms of performance, would not provide significant weight reduction.

Design considerations for the 3 km/s shields were obtained from a number of sources. Conventional ballistics research contains performance data, material specifications, and theories concerning the interactions between the two front plate layers of an A/B type shield (Goldsmith and Finnegan, 1971; Wilkins et al., 1969; Nicol et al., 1988). Further information came from ORNL ballistics research into areas concerning sub-layering, different materials, and plate interaction (Brewer, in press). Previous ORNL hypervelocity shielding experience (ORNL staff, 1989) was utilized in the front plate phenomenology and also in the carbon felt disrupters and the 21-6-9 back plates. The analytical work, discussed in Sections 6 and 7, provided material comparisons, spacing information, and interest in the use of wire mesh plates. Series 7 tests used information obtained from the tests of Series 6. Shields 69, 71, 72, 73, 79, 80, and 81 were based

on the A/B plate ideas, with shield 78 using the wire mesh concepts. Spaced front shields were not tested, having shown no advantage in the analytical work. Material availability was also a consideration in shield design. "Off-the-shelf" materials were used as much as possible.

Ideally, in a successful layered shield the energy of the incoming projectile would be distributed appropriately throughout the shield components, with each layer being completely utilized. With several layers in a shield, the function and interaction of the different layers need to be well understood for optimum shield design, both for performance and for weight reduction. For the low velocity threat, design of the front shield is especially important, as much of the weight of the shield is located in the front plate. This is especially true of the A/B type front plates and for the 3 km/s shields in general. From examination and comparison of the 7 layered configurations tested, the performance of each layer and the energy distribution is discussed below. The following characteristics of each test result are used as performance indicators:

> front plate ejecta produced, front plate hole size and amount of fracturing, debris found in the disrupter layers, spread of the blast damage in the disrupter layers, time from front plate impact to the impact of debris on the back plate, back plate damage, and witness plate damage.

The time from initial impact on the front plate to the time at which debris begins to impact the back plate is given in Table 2. All available debris travel versus time information, obtained from flash x-ray data, is summarized in Table 3. The debris travel distances given are the distances from impact and include the front plate thicknesses. Travel times, given the fact that all the shields had the same disrupter, are indicative of the front shield performance in two ways: (1) the time of projectile/front shield interaction and (2) the velocity reduction of the resulting debris behind the

Table 3. Debris cloud travel versus time information

	debris travel distance and time, from impact					
	x-ray 1		x-ray 2		back plate	
Shot no.	cm	μsec	cm	μsec	cm	μsec
69	4.1	18	-	-	15.24	254
71	-	-	-	-	15.24	271
72	3.2	14	-	-	15.24	263
73	-	-	-	-	15.24	447
78	9.7	43	14.3	78	15.24	82
79	6.5	49	9.6	84	15.24	205
80	6.3	43	9.7	78	15.24	184
81*	6.8	22	-	-	15.24	95±3

*Test performed at 7 km/sec

front shield. Generally speaking, longer travel times indicate the front shield was more effective and vice versa. However, too much front plate can also be indicated by an extremely long travel time. The short time of test 81 should not be evaluated in the same manner as the remaining shots due to the impact velocity difference.

In discussing shield 69, several points are of interest. The A layer, while it had a large hole, was not fractured at all, and there was very little ejecta produced. Significant amounts of the incoming energy can be converted to kinetic energy of ejecta, with smaller amounts expended in fracture energy (Nicol et al., 1988). For this shield, almost no energy was absorbed this way. The B shield was somewhat dished back, with a large, axisymmetric hole produced; i.e., the front side was smooth, with no lip, while the exit side of the plate was extended into a tapering lip. This exit lip was slightly turned outward but not enough to describe as petaled. The exit side of shield 69's B plate is shown in Figure 19. From Thomson (1955), this type of hole requires 2.66 times less energy to produce than a symmetric hole having a material lip formed upon both the entry and exit

ORNL PHOTO 8256-89

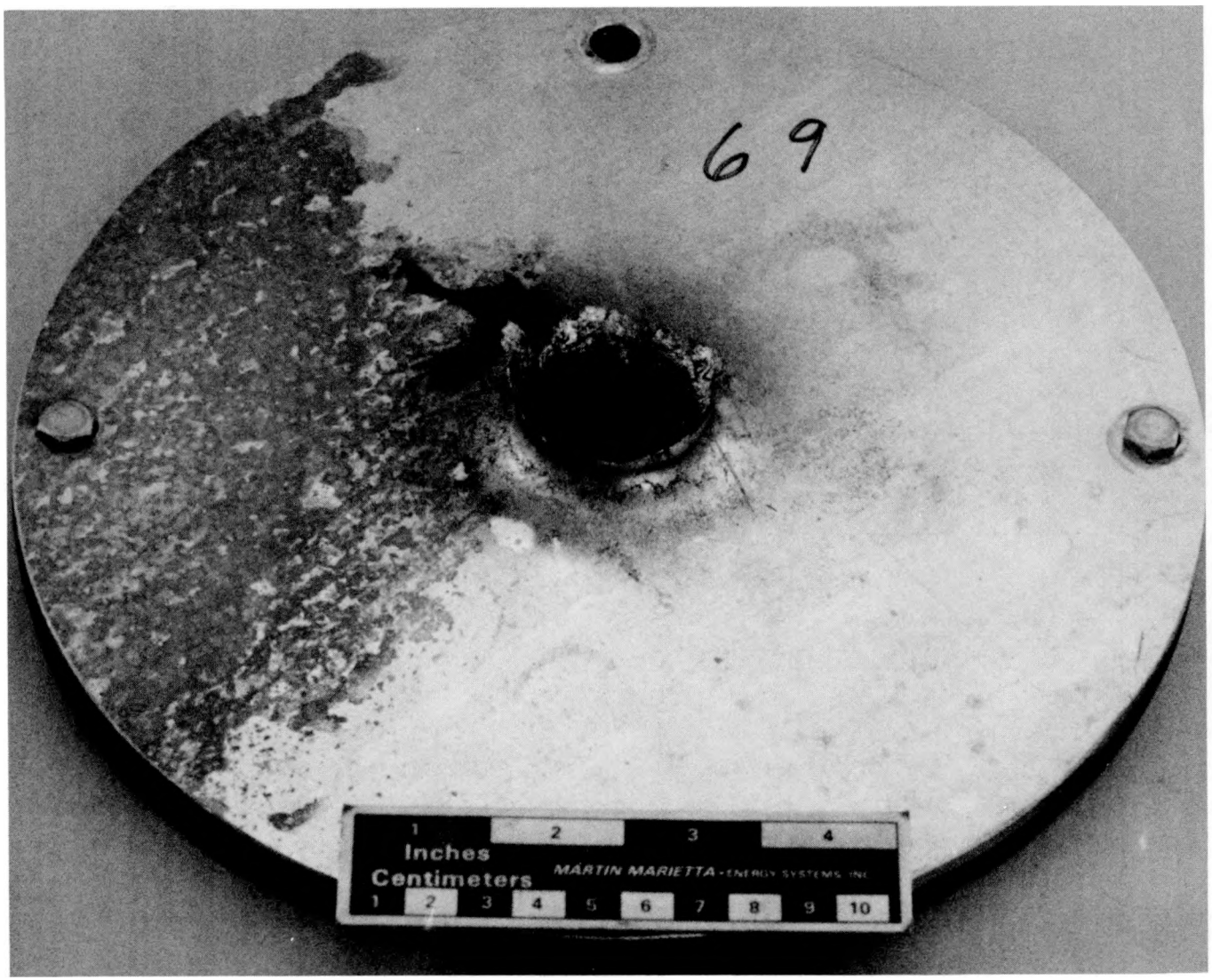

Figure 19. Shield 69 B layer, exit side

sides, as characteristic of the hypervelocity impact front plate holes. The axisymmetric hole is very typically found in backup plates used in ballistics testing. However, the energy expended in forming this type hole is significant, with incoming kinetic energy being used in the bending of the plate (Nicol et al., 1988). The creation and velocity of spall particles found in the disrupter layers also used a significant amount of energy. This energy was absorbed partly by the disrupter, from the large number of particles found in the layers and partly by impact on and deformation of the back plate. The shape of the blast profile in the disrupter is significant in that it is most similar to the shape of the blast profile for shield 78 (both are shown in Figure 12). Shield 78 did not have an A layer; the projectile impacted directly onto a metal surface. The similarity between the two, combined with the fact that shield 69 has the shortest travel time of the three setups with identical B plates, indicated that the A plate for shield 69 was not particularly effective. The disrupter layers were effective in slowing and stopping significant amounts of debris. Also, the back plate completely stopped all impacting debris and was not seriously deformed, indicating at least some degree of underutilization.

Results for shield 71 were similar to those for shield 69 in some ways. The type of hole formed in the B plate is very similar with the hole for 71 being just slightly smaller. The B plate for shield 71 is shown in Figure 20 from the exit side. Again, the disrupter was effective in stopping significant amounts of debris. The back plates were also very similar in the amount of energy absorbed. However, major differences can be seen in the front plates and there is a noticeable difference in the shape of the blast damage profile in the disrupter. The A plate was extensively fractured, especially in the region around the hole, with a significant amount of ceramic ejecta produced. This indicates that more energy was used in penetration of the A layer. The similar performance of the B layers is expected as they are identical in both material and thickness.

Figure 20. Shield 71 B layer, exit side

Another indicator of the improvement in A layer performance is the increased time before back plate impact.

The A plate results for shield 72 were similar to those of shield 71, since both shields used the same type A plate. Less fracturing and less outward ejecta were produced by shield 72. While less ceramic debris was produced overall, more of the ceramic debris traveled into the shield. Thus a significant amount of kinetic energy was transferred to plate debris, but the travel direction differed. The disrupter and back plates were again quite effective, if possibly underutilized. A note of interest concerning shield 72 is the "ring" of damage from the lead found in the disrupter, referring again to Figure 12. This corresponds well with the hypervelocity work of Piekutowski (1987), who reported on the debris cloud material distribution from hypervelocity impact. Material from the front shield would be expected in the outer regions of the blast damage, which is where the lead fragments were found. In evaluating the relative performance of the shield components, the lead B plate did not perform as well as the aluminum plates, despite its equal areal density. The soft, weak lead allowed the ceramic to break away from the projectile rather than forcing the projectile to fracture, compress, and travel through the ceramic. This point is further supported by the fact that the travel time for shield 72 is less than for shield 71 and approximately the same as for shield 69. The lead plate was not dished to any significant degree with relatively little energy absorbed in this way. The exit side of the lead hole also differed from the aluminum plate results, having a lip that had curled around until it could be described best as petalled. This is shown in Figure 21.

Test results for shield 73 were quite different in several ways. The A layer, consisting of four thin sublayers, was completely shattered into tiny fragments. These fragments were scattered

ORNL PHOTO 8240-89

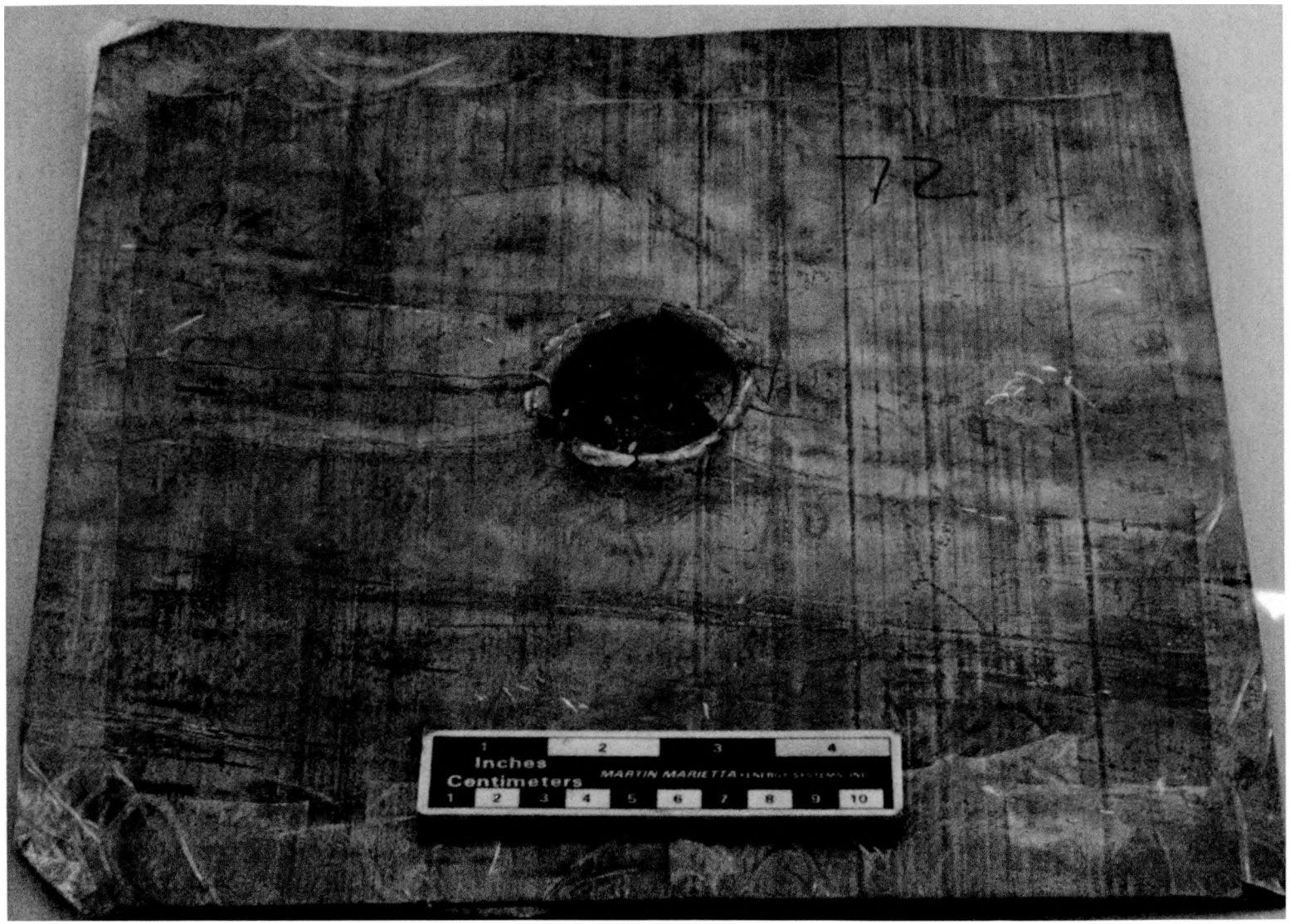

Figure 21. Shield 72 B layer, exit side

widely. This phenomena undoubtedly used a large amount of the incoming kinetic energy. The B plate damage was different from any of the other shields. The plate was very definitely dished, and the hole produced had a long, tapered exit lip with absolutely no outward flare or indication of incipient petalling. This is shown in Figure 22. Also shown in Figure 22 is the single large piece of spall produced from the B plate impact. All disrupter and back plate damage was produced by this spall. From the extremely long time to back plate impact, the spall was moving very slowly. These results indicate that the primary absorption of energy was in the front plate phenomena. Since the B layers were the same for shields 69, 71, and 73, this also indicates that the A layer was the factor causing these results. The increased thickness of the A layer probably also contributed to the very long time before back plate impact. With a material and thickness change, as well as the possible effect of the sublayers, the different performance of shield 73 is expected but which of these differences contributed to which specific result is not fully defined.

Recent results from armor/anti-armor research programs at Los Alamos National Laboratory (Sandstrom, 1989; Mah and Martell, 1989) indicate that the action of the ceramic layer in actually grinding up the projectile, rather than flattening the projectile and spreading out the damage area, is more important in shield success. Their results also indicate an improvement in performance from confining the ceramic, so that the projectile does not move the ceramic out of the way but is instead forced to compress and move through the material. This confinement also increases the grinding effect. An improvement in ballistics shielding due to sublayering had been previously noted in ORNL ballistics research (Brewer, in press), and it may well be that these effects are related, with the different layers serving to confine the material and force greater utilization of the ceramic. However, the material differences effect remains as a question to be answered. These

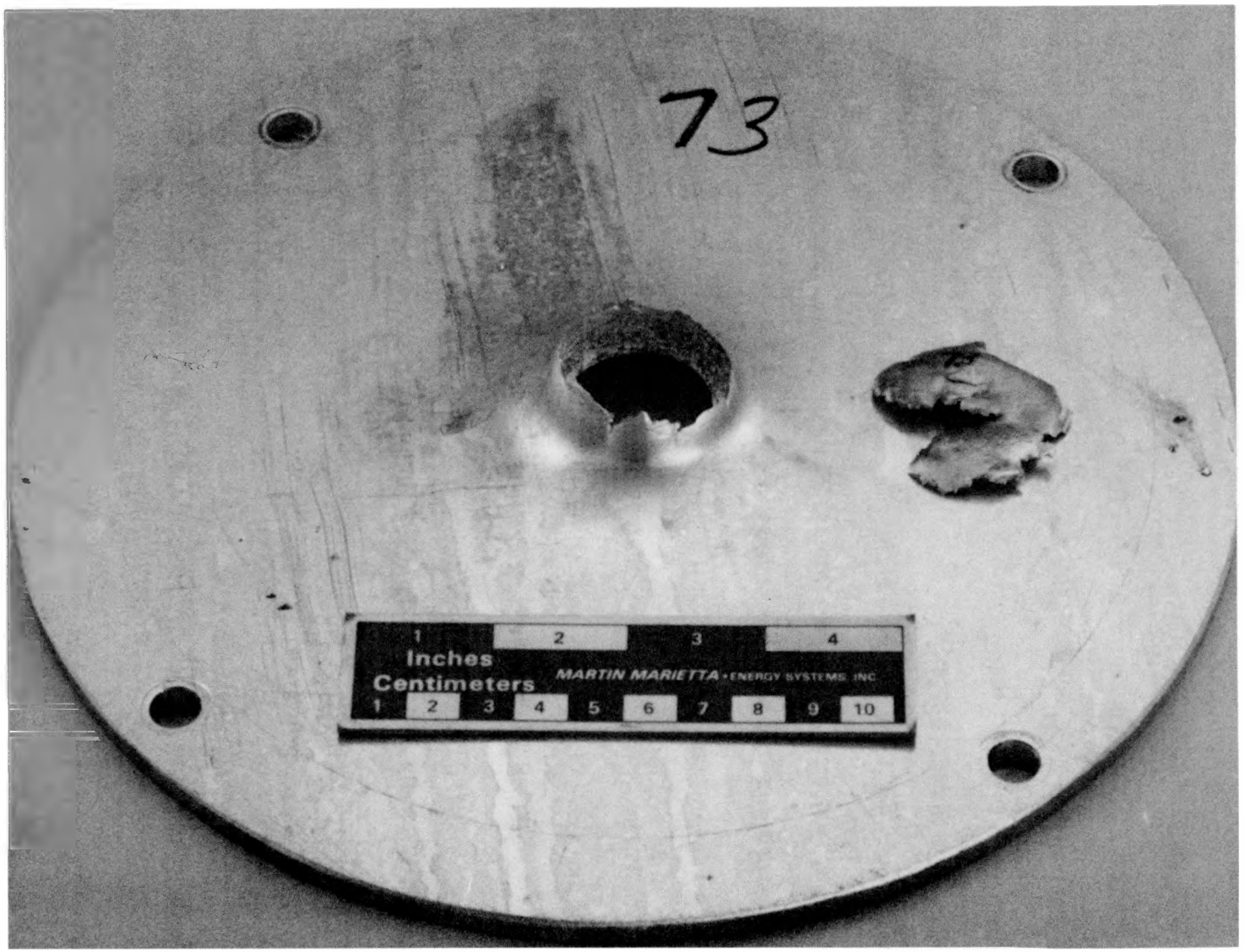

Figure 22. Shield 73 B layer, exit side, and spall fragment

results are promising, in terms of indicating areas for further research, but the limited amount of data precludes any definite conclusions in this area.

From the analytical work, a wire front shield was indicated as a likely candidate for weight reduction. Shield 78 was less than 30% of the reference weight. However, the wire front shield was not entirely effective. Some amount of the projectile was broken up well, as can be seen from the widespread blast damage in the disrupter and the scattered small bulges on the back plate. Unfortunately, a significant portion of the projectile appears to have remained intact, as there is a clear hole straight through the disrupter, the back plate, and the witness plate. The debris cloud was traveling at a high velocity, even faster than for shield 81, which was tested at a 7 km/s impact velocity. This can be seen from the distance versus time information of Table 3. The flash x-ray data for shot 78 is shown in Figure 23. These x-rays also show the projectile debris breakup/incomplete breakup combination previously discussed, as well as providing the travel versus time information.

The shield appears to have been impacted with the projectile axis yawed significantly. This is apparent since five wires were damaged rather than the three that would have been impacted had the projectile hit perfectly orthogonal to the front surface. Also, as can be seen in Figure 24, on the exit side of the plate there are wires moved back into the disrupter layers. This might be due to a yawed impact or could be caused by exiting debris/spall. Again, data are limited. The effect of using a cylindrical rather than a spherical projectile on the shock wave interaction has not been studied. The yaw angle of the cylindrical projectile could also be expected to affect the shock wave interaction, but again, this has not yet been studied. With a limited amount of analysis and an

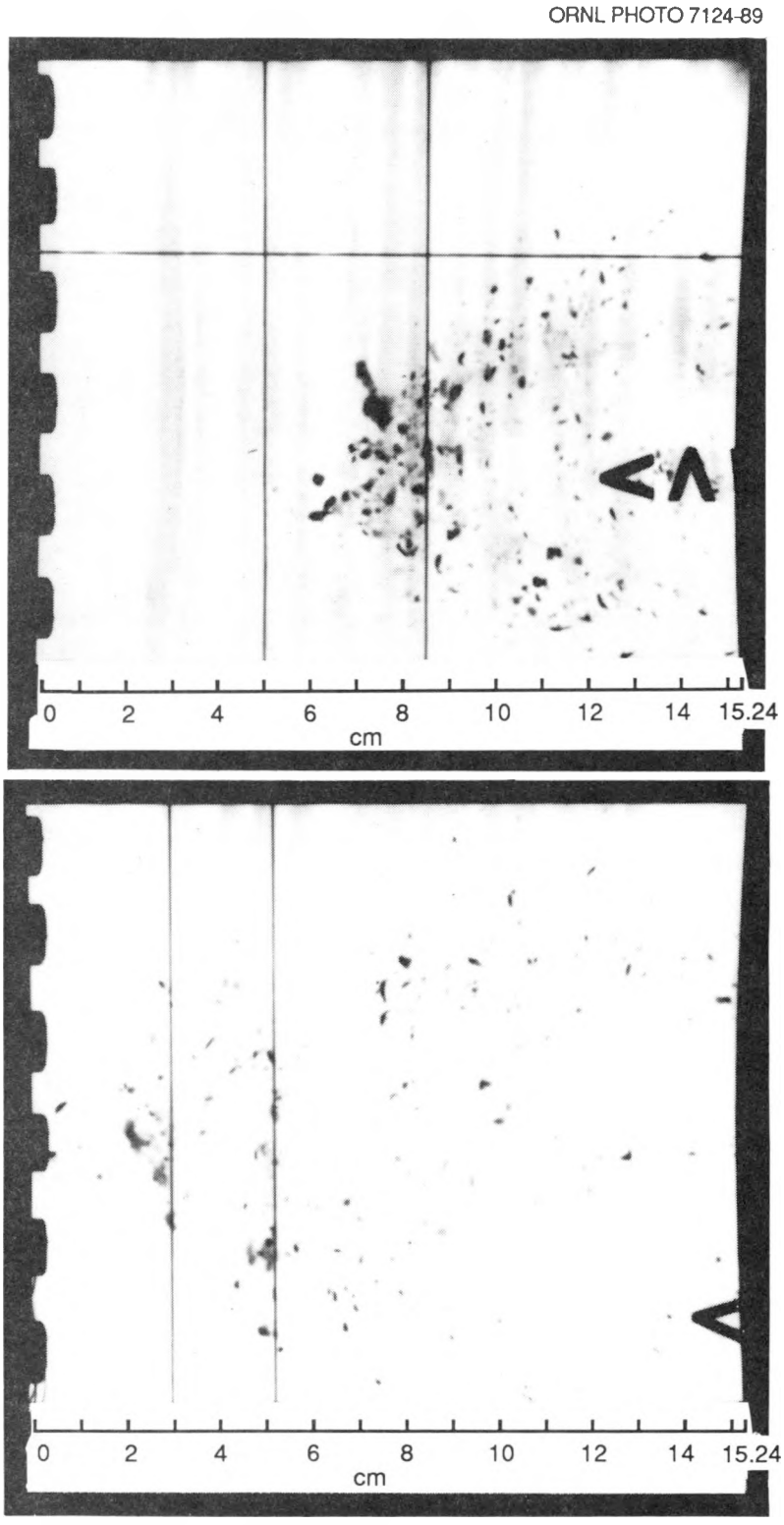

Figure 23. Flash x-ray data for shot 78 at 43 and 78 μsec

ORNL PHOTO 8237-89

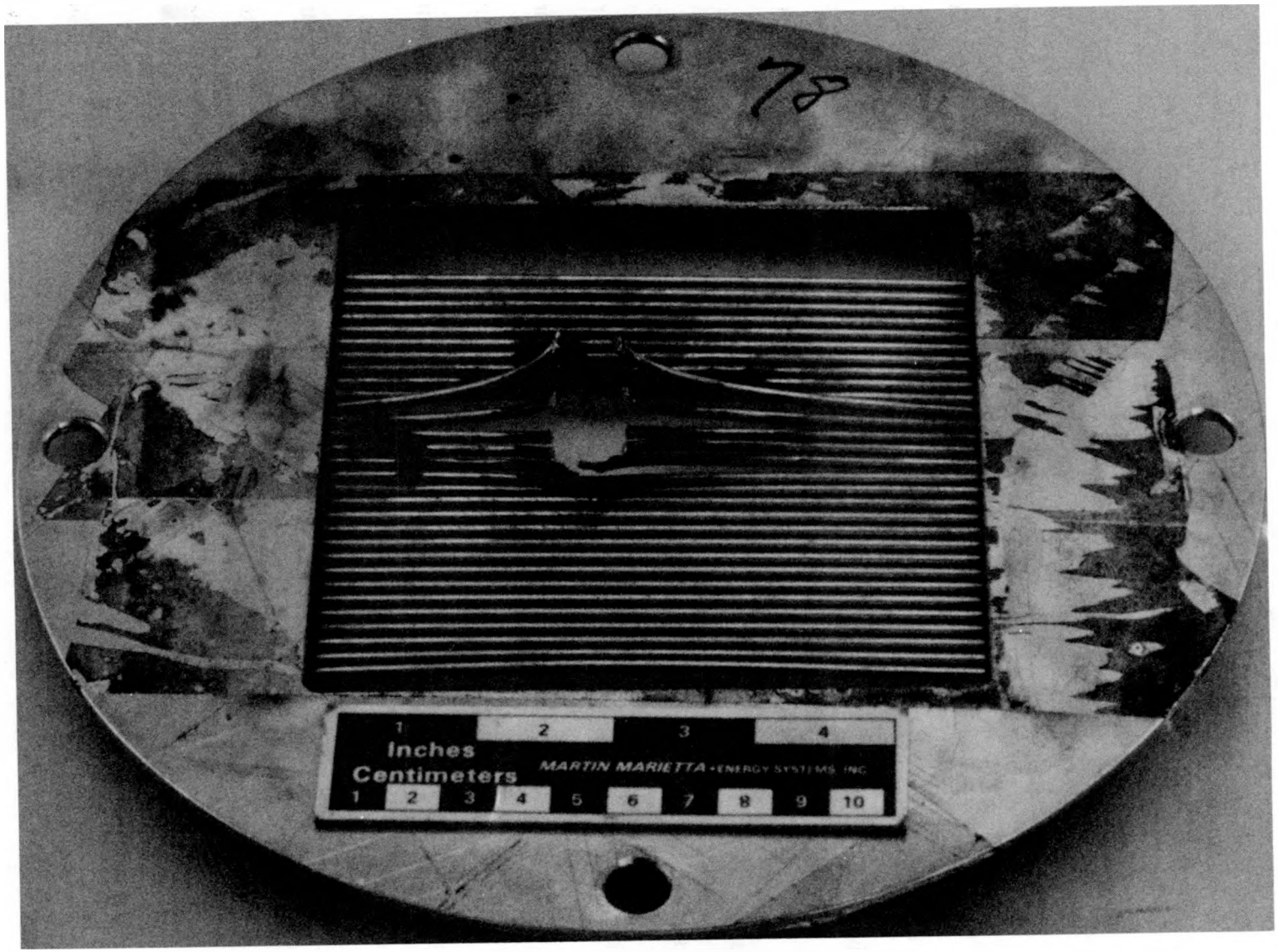

Figure 24. Shield 78 front plate, exit side

even more limited amount of testing using wire front shields, the failure of shield 78 is not a clear indicator of general wire shield performance.

Shield 79 was an A/B type front plate stackup. Both front plate layers are shown in Figure 25 with the entry side of the A layer and the exit side of the B layer visible. The A layer was damaged over a relatively small area, and there were essentially no ejecta. The B layer was only very slightly dished, unlike the previously tested B layers. The disappearance of dishing corresponds to an increase in projectile speed (Goldsmith and Finnegan, 1971). Since the initial impact speed was the same, the projectile velocity was reduced less across the A layer of 79 than the other A layers tested. This phenomenon is also evident by the axisymmetric appearance of the hole in the B layer, as the hole has a definite lip on the entry and exit sides. The exit hole lip is no longer extended and tapered as in the previously discussed plates. The exit hole side lip is more irregular than the entry side, having debris particles only partially separated still on the rim. The appearance of the B layer indicates the projectile debris penetrated the B layer at a higher velocity than for the previous shield B layers. Also, the axisymmetric type hole formed required more energy (Thomson, 1955). The disrupter layers again were effective in slowing and stopping significant amounts of debris, as was the back plate. The travel time from front to back impact was less than for the four previously tested A/B type shields, which all had both thicker and heavier A and B plates. A complete set of flash x-ray data was obtained for shot 79 and is shown in Figure 26. These data for distance versus time, also in Table 3, indicate a good velocity reduction across the front plate. Large pieces of high density debris are visible, matching the aluminum debris fragments found during posttest disassembly. The A/B combination used was effective, but the individual contributions of the two layers are not well defined. A significantly greater amount of energy was absorbed by the B plate, as previously discussed. However, the travel time for shield 80, which had

ORNL PHOTO 8238-89

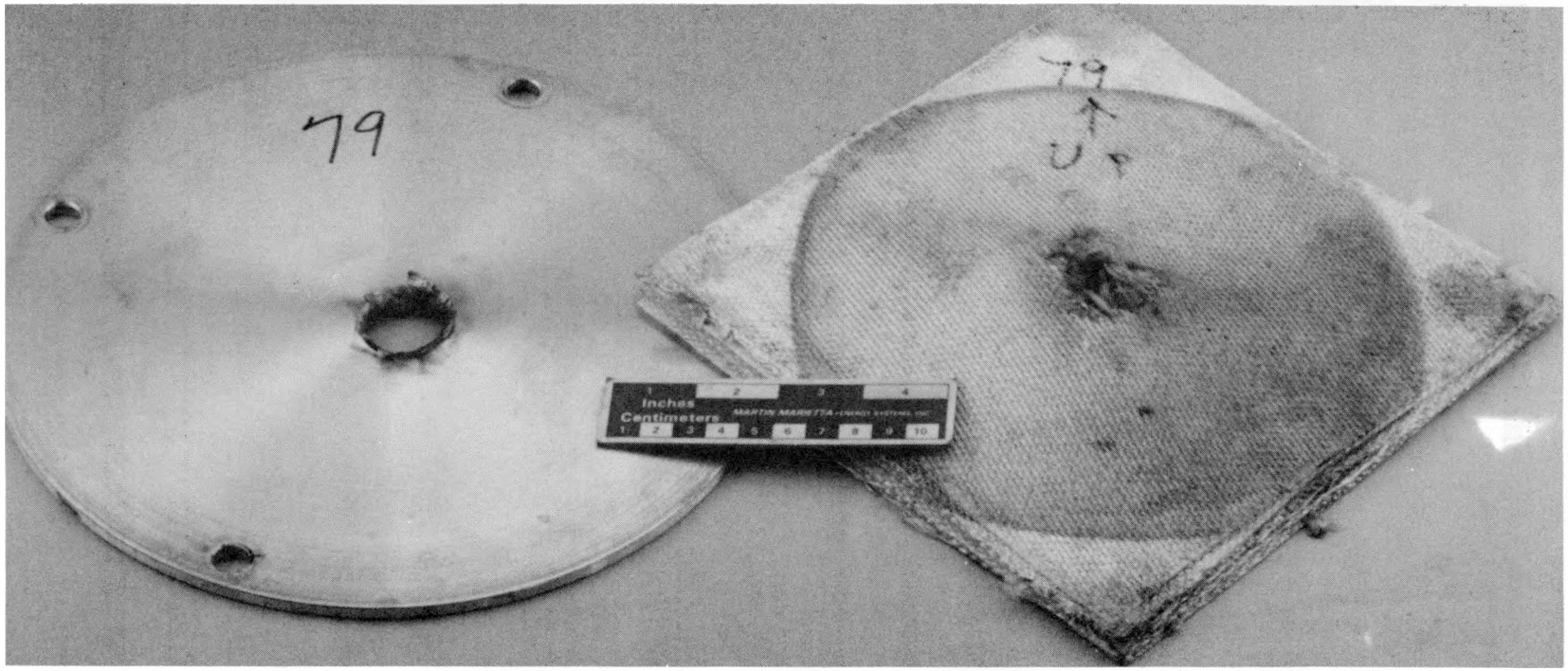

Figure 25. Shield 79 A layer, entry side, and B layer, exit side

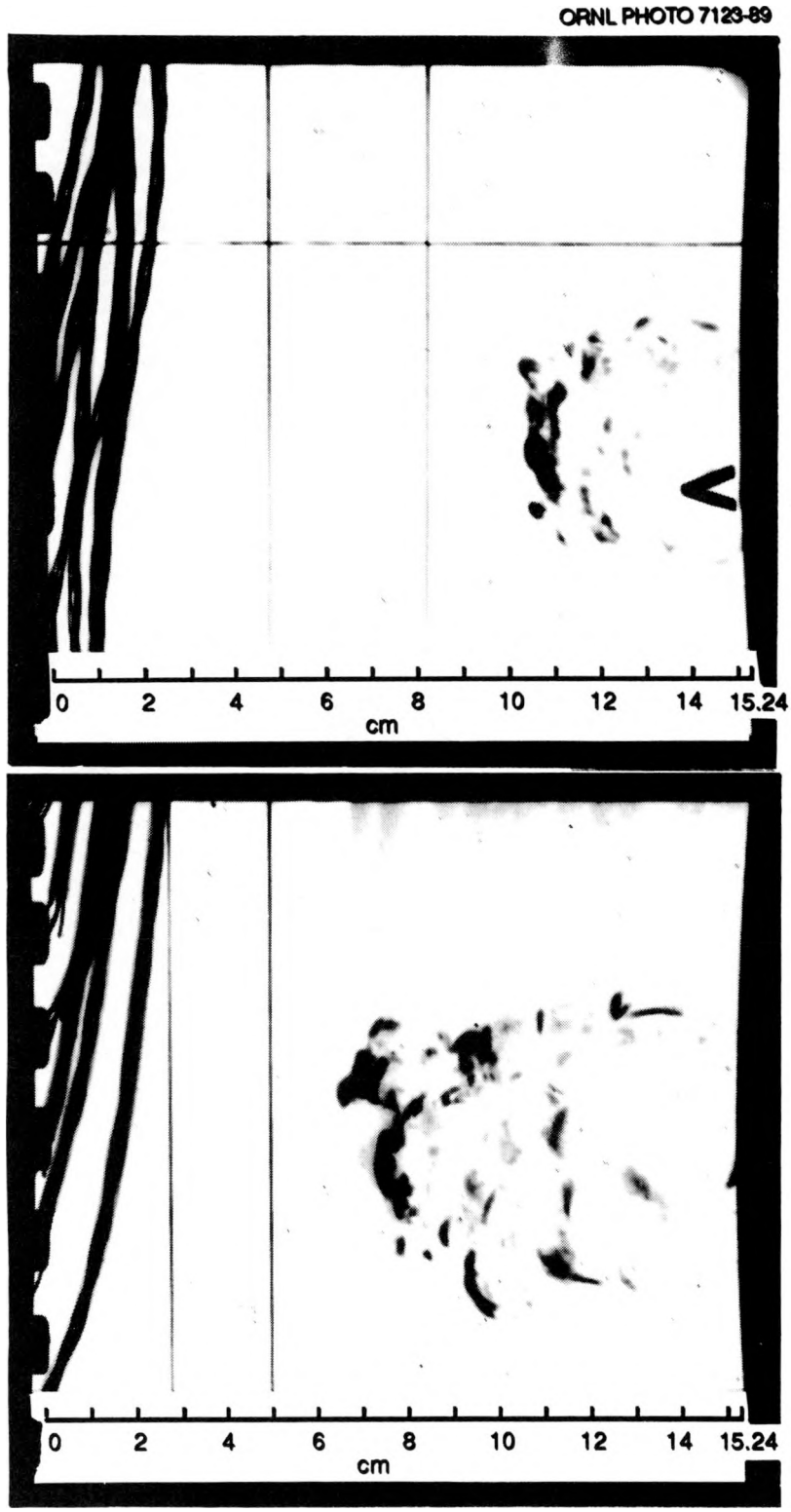

Figure 26. Flash x-ray data for shot 79 at 49 and 84 μsec

an identical B plate, was less than for shield 79, which indicates the A layer also contributed to the success. Shield 79 was the lightest of the successful shields, having a weight reduction down to 41.50% of the 3 km/s reference shield.

The A plate of shield 79 is of interest due to the successful performance of this shield and the very low amount of ejecta produced. While transferring significant amounts of projectile kinetic energy to ejecta kinetic energy is a positive factor when looking at the likelihood of shield success, the large amount of debris ejected into the immediate vicinity is a definite overall drawback of the ceramic plates. The ceramic cloth used in the sublayered A front plate is of interest in that performance was maintained while ejecta were greatly reduced. Referring again to the recent Los Alamos results concerning grinding and confinement effects (Sandstrom, 1989; Mah and Martell, 1989), the ceramic cloth success may be related to similar factors. However, these results also indicate a need to test confined solid ceramic plates, which could significantly help in confining the debris produced.

The A/B front plate of shield 80 was a solid ceramic and aluminum combination. To evaluate the effect of the shock of impact on a tiled shield structure, the ceramic layer of the shield was composed of small separate ceramic tiles. The ceramic tile actually impacted was severely fractured and jarred loose. The tiles that were not directly impacted were less severely fractured but most of the fragments were also jarred loose. This result is important in the further evaluation of the ejecta/debris generated, as discussed above. Possibly a different tile configuration or bonding would be affected less severely; this effect has not been investigated fully.

In the evaluation of the different layers of shield 80, the A layer, as mentioned previously, was very fractured and considerable ejecta were produced using projectile energy in the process. The B plate, shown on the exit side in Figure 27, was very definitely dished and had no lip on the entry side, with a small, tapered lip on the exit side. The combined effect of this A/B plate configuration was not as effective as that of the previous shield. This can be seen from the flash x-ray data and the back plate failure for shield 80. Flash x-ray data for test 80 is shown in Figure 28 and in Table 3. These data show the lesser velocity reduction and slightly higher density debris for shot 80 as compared to shot 79. Considering the energy distribution and layer utilization of shield 80, it is thought that the A layer was too heavy, either too thick or too dense, and that a performance improvement would result if the A layer were lessened. This would shift more of the load to the B plate and thus use it more effectively, while also reducing shield weight. Again, the disrupter and back shield were effective; the back shield was overloaded due to the front plate configuration. Increasing the back shield would also improve this configuration's performance but would be inefficient in terms of weight.

According to previous research on the projectile velocity effect on layered shield effectiveness, as shown in Figure 17, a shield that is successful against a 3 km/s threat should be successful against the same threat at 7 km/s, since damage level at 7 km/sec is much lower. The results of Figure 17 are for tests using identical front shields and measuring back plate damage. However, the effect of a too-thick single-layer front shield is known to be damaging at the 7 km/s velocity (ORNL staff, 1989), and dual plate front shields have not been extensively studied at the higher velocity. For these reasons, the lightest of the successful shields against the 3 km/s threat was tested against the same projectile at 7 km/s. This was shield 81. The weight reduction for the same shield stackup but a different reference shield was considerable, down to 16.7%. This is in comparison to the

ORNL PHOTO 8257-89

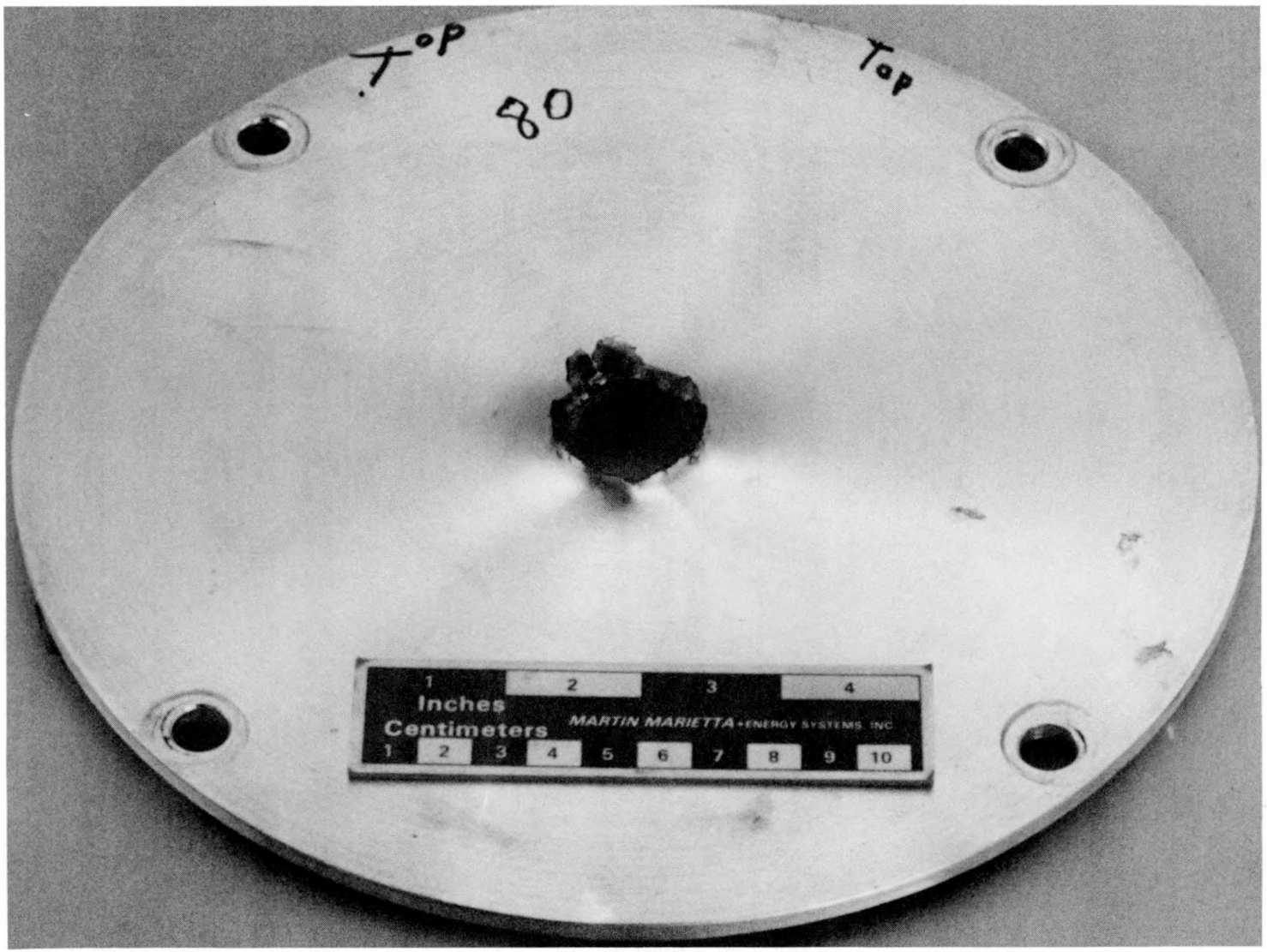

Figure 27. Shield 80 B layer, exit side

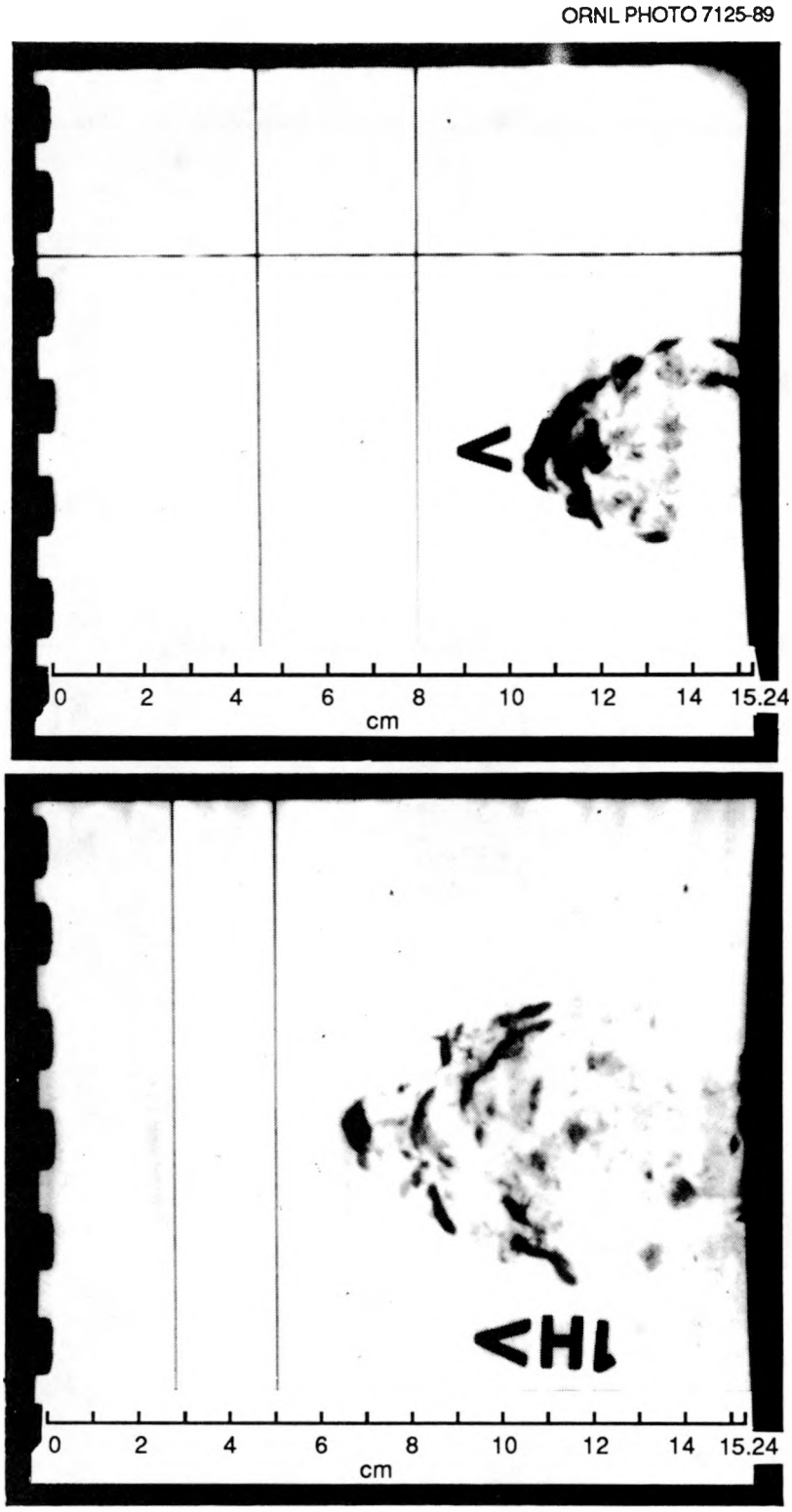

Figure 28. Flash x-ray data for shot 80 at 43 and 78 μsec

41.5% of the 3 km/s reference, illustrating the point previously discussed concerning one of the difficulties of weight reduction for the 3 km/s threat. In comparison, the lightest weight shield (shield 41) achieved for the case of the 7 km/s aluminum threat was 10.62% of the 7 km/s reference solid shield, with an overall areal density of 2.273 g/cm^2 (Thomas et. al., in press). Shield 41 is 26.3% of the 3 km/s reference, but would be highly unlikely to stop the 3 km/s aluminum threat. This phenomenon is discussed more completely in Sections 7 and 9.

Comparing shield 81 with shield 79, the damage to the A and B layers of shield 81 was much greater than for shield 79. The entry side of the A layer and the exit side of the B layer are shown for shield 81 in Figure 29. The greater level of damage can be seen by comparing Figures 25 and 29. A much larger hole with significantly more frayed cloth surrounding it was produced in the A layer of shield 81. In the B layer, the hole was also much larger than for shield 79. The appearance of the B layer holes was quite similar. The lip on the entry side of the B layer of shield 81 was more pronounced, and there was no dishing at all. These phenomena correspond to the higher velocity and energy level of the 7 km/s projectile. In the disrupter layers, the blast was much more spread out, as shown in Figure 12. The blast did more damage to the disrupter layers with large sections blown completely out of the shield 81 stackup. Flash x-ray data for shot 81 is shown in Figure 30. From this data point and the back plate data for travel versus time, the debris cloud was definitely traveling very rapidly, in comparison with the debris cloud of shot 79 (Table 3). However, the velocity reduction across the front plate was quite large, as a typical travel time for a successful 7 km/s shield is approximately 50 μsec, versus 95 μsec for shield 81. By comparing the debris cloud for shot 81 (Figure 30) with the debris cloud for shot 79 (Figure 26), it can be seen that the debris in the high velocity cloud of shot 81 is generally of lower density. The back plate was more bulged overall, indicating a significant blast wave loading.

ORNL PHOTO 8236-89

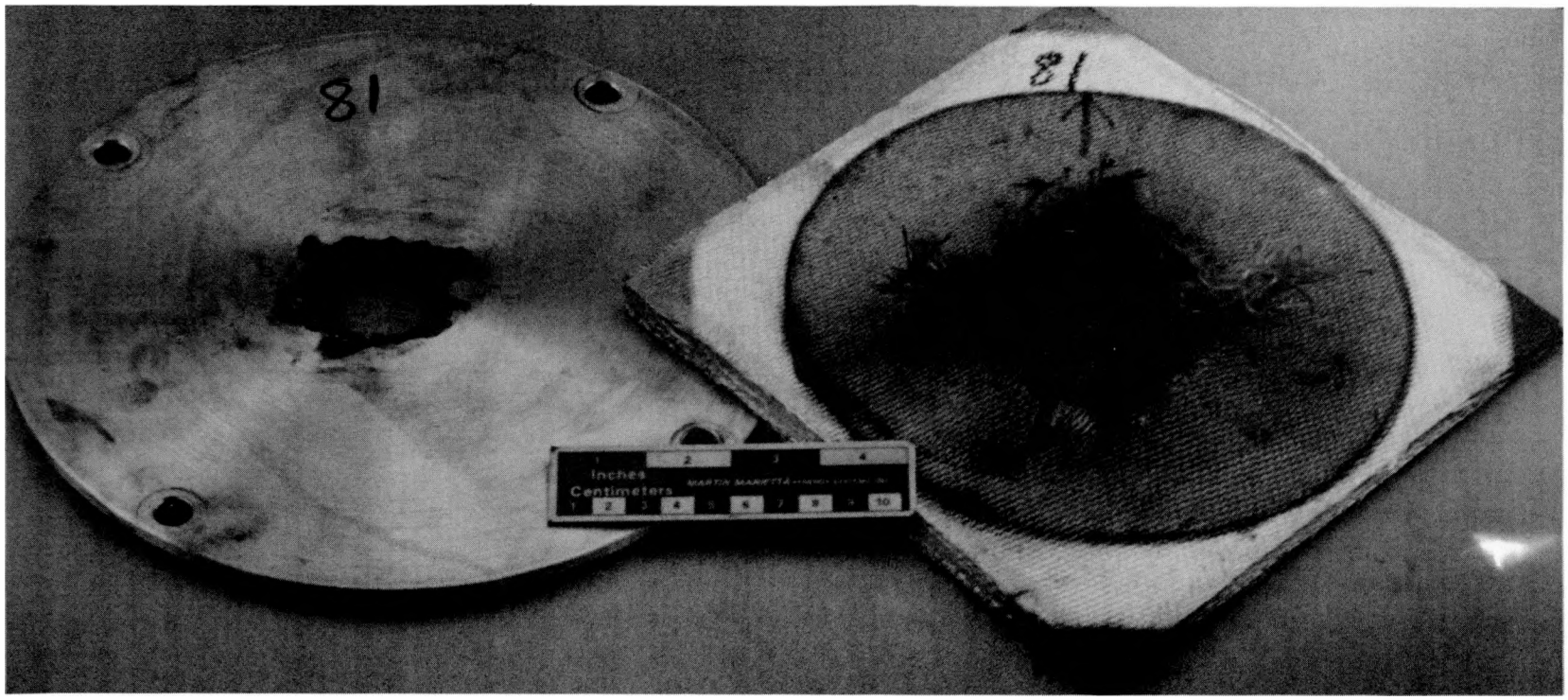

Figure 29. Shield 81 A layer, entry side, and B layer, exit side

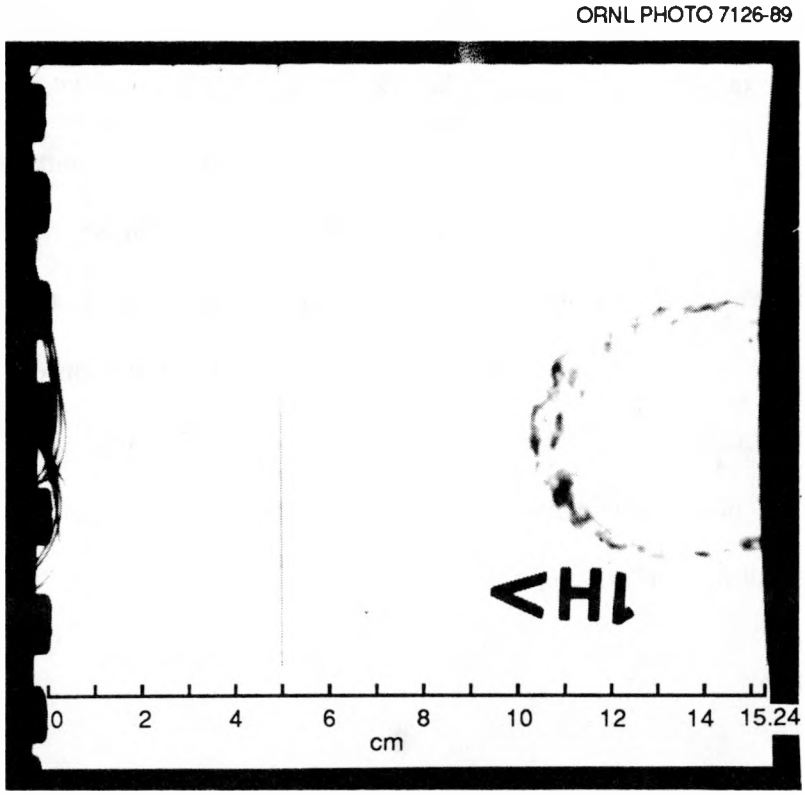

Figure 30. Flash x-ray data for shot 81 at 22 μsec

The damage to the shield was extensive, even though the back plate did not fail. This indicates caution should be used in applying the damage curve of Figure 17. The variation in the front plate configuration is very important and could more than override the lesser damage potential.

Shield results cumulatively indicate a tradeoff in performance between the different layers. In shield 73, the increase in the A layer was sufficient to almost overload the back layer, indicating an improvement in weight with no loss in performance could be obtained by lessening the A layer. The results of shield 78 show that an insufficient front plate requires more back plate for success. An optimum front plate combination would allow for utilization of the back plate, while too much or not enough front plate appears to increase the back plate required. Similarly, there is an

interaction between the A and B layers with different combinations yielding equivalent performance. For example, comparing shields 69, 71, and 72, the ceramic layer in shield 72 was much more effective than the lead. In shield 69, the aluminum layer contributed more than the K-Karb. For shield 71, the two layers appear to have contributed approximately equivalently. However, from the similar travel time and back plate appearance for the three shields, the three A/B combinations are not significantly different. The function of the different layers is not yet completely understood, but from the results at this time, the A/B layers and their interaction are extremely important in the low hypervelocity area. A better understanding of the front shield phenomena would allow further weight reduction.

6. ANALYTICAL CONFIGURATIONS

The analysis effort was devoted entirely to front plate phenomenology, as past experience had shown that effective projectile breakup by the front plate is essential for a successful shield design. Very large displacement of localized areas, including penetration and ejecta, requires that a hydrodynamic computer code or hydrocode be used. The hydrocode makes use of finite difference methods to approximate the solution of the governing partial differential equations. These equations are based on the conservation of mass, momentum, and energy, along with an equation of state and constitutive relationships to properly model the material behavior.

The Eulerian based version 120.2 of the Hull (Matuska and Osborn, 1987) hydrocode was chosen to model the projectile and front plate impact. The Eulerian version has a framework of cells fixed in space through which material flows. Consequently, very large deformations do not require a remesh or restart as in the Lagrangian or material fixed coordinate systems. The Hull computer code has been widely used in impact studies for a large range of velocities and for a variety of materials. Correlations with experimental data were good for the lexan projectiles studied in the first phase of this program as reported in the Fast Track Progress Report (ORNL Staff, 1989).

Material properties are key parameters in the successful modeling of a hypervelocity impact event. (Stability criterion for the explicit integration scheme is also quite important.) The Mie-Grunieson material model was used to represent the projectile and the front plate. Appropriate values of ultimate strength and strain were used from tests at high strain rates. The disrupter material was modeled as a gas of appropriate density. This procedure has correlated well with experimental data in the past (ORNL Staff, 1989), since mass effects are the primary consideration.

Nineteen different impact configurations were studied as part of the low hypervelocity phenomenology effort. These can be divided into subgroups indicative of the phenomena being analyzed. All nineteen problems are summarized in Table 4, which includes projectile and front shield information and a brief results description.

The first group, consisting of problems 2.5, 2.52, 2.35, and 3.52, used shield configurations previously seen to be very effective at the 7 km/s impact velocity. Spherical projectiles were used (ORNL Staff, 1989). Problem 2.5 modeled a lexan projectile and aluminum front shield combination; problem 2.52 modeled an aluminum projectile and stainless steel front plate combination; and problem 2.35 modeled a tungsten projectile and stainless steel front plate configuration. Problem 3.52 was a repeat of problem 2.52 but with aluminum properties adjusted to more realistic values.

The next eight problems studied, numbers 4.52 through 2.25, incorporated different materials and thicknesses of front plates, in an attempt to find an effective configuration for good projectile breakup. Alternate materials were chosen for the front plate to gain increased strength and volume density. Four of the problems in this group (5.52, 4.42, 3.42, and 7.52) also modeled the effect of velocity changes from 2.5 km/s up to 4.0 km/s.

In the next three configurations, two ceramic plates were used, together having an equal areal density to that of a previously modeled configuration. Three very close spacings between the plates were chosen to provide impact with the second plate either during or after compression wave travel in the projectile. All other parameters were held constant.

Table 4. ASP study of composite front plates

Problem Nos.	PROJECTILE SPHERES Material	Areal density g/cm²	Dia., cm	Proj g/cm²	FRONT PLATE/WIRE Matl	Thickness cm	Areal density g/cm²	Plate g/cm²	Proj	Velocity km/sec	Velocity at 15 μsec km/sec	Projectile Breakup
1) 2.50	Lexan	1.18	1.48	1.16	Alum	.16	2.71	.434	.374	2.50	1.75 (10 μsec)	Poor
2) 2.52	Alum	2.71	1.12	2.03	SSteel	.16	7.86	1.26	.62	2.50	1.56	Poor
3) 2.35	Tung	18.1	.60	7.19	SSteel	.24	7.86	1.89	.262	2.50	2.03	Very Poor
4) 3.52	Alum	2.71	1.12	2.03	SSteel	.16	7.86	1.26	.62	2.50	1.54	Poor
5) 4.52	Alum	2.71	1.12	2.03	Ceramb	.16	3.9	.624	.31	2.50	1.83	Poor
6) 4.52(R)	Alum	2.71	1.12	2.03	Ceramb	.32	3.9	1.25	.615	2.50	1.40	Poor
7) 5.52	Alum	2.71	1.12	2.03	Ceramb	.32	3.9	1.25	.615	4.0	2.35	Excellent
8) 4.42	Alum	2.71	1.12	2.03	Ceramb	.16	3.9	.624	.31	4.0	2.86	Good
9) 6.52	Alum	2.71	1.12	2.03	Tungsten	.16	18.1	2.90	1.43	2.5	1.03	Fair
10) 3.42	Alum	2.71	1.12	2.03	Ceramb	.16	3.9	.624	.307	3.25	2.41	Poor
11) 7.52	Alum	2.71	1.12	2.03	Ceramb	.16	3.9	.624	.307	3.00	2.22	Poor
12) 2.25	Alum	2.71	1.12	2.03	Tungsten	.08	18.1	1.45	.71	2.50	1.52 (13.5 μsec)	See 6.52
13) 2.42	Alum	2.71	1.12	2.03	Ceramb Cerams*	2 @ .16	3.9	Total= 1.24	.611	2.50	1.24	Poor-space 1/2+1/3
14) 2.422	Alum	2.71	1.12	2.03	Ceramb Cerams*	2 @ .16	3.9	Total= 1.24	.611	2.50	1.28	Poor-space .35+3.65
15) 2.423	Alum	2.71	1.12	2.03	Ceramb Cerams*	2 @ .16	3.9	Total= 1.24	.611	2.50	1.39	Poor-space .17+3.83
16) 9.112	Alum	2.71	1.12	2.03	Alum	.28**	2.71	.298	.147	2.0	-	Poor-wide spacing
17) 9.15	Tantalum	16.6	0.613	6.79	Tantalum	.15**	16.6	1.31	.193	2.0	1.75 (12 μsec)	Good-narrow spacing
18) 9.16	Alum	16.6	1.12	2.03	Alum	.28**	2.71	.397	.196	2.0	-	Good-narrow spacing
19) 7.32	Alum(cyl.)	2.71	0.94	2.55	SiO_2/Alum	1.034/ 0.335	2.20/ 2.71	3.18	1.25	3.06	0.68	Good

*Ceramb same material as cerams; labeled for sorting purposes
**Wire diameter

For problems 9.112, 9.15, and 9.16, a more unconventional front plate configuration was chosen. The spherical projectile was impacted into a front plate composed of closely spaced wires. Wire size and spacing were chosen to ensure projectile contact with three wires, even though the leading edge of the spherical projectile would encounter the center wire before the outer two. Wire diameter was set at one-fourth the projectile diameter, and two different spacings were studied.

The final analysis configuration, problem 7.32, was an attempt to model test 73. All parameters were set up as closely as possible with the known conditions of shot 73. One difference is in the layering of the A front plate, which for shield 73 was composed of four thin layers. Cost and time constraints prohibited the inclusion of very small air gaps to model the sublayers. In problem 7.32, the A front plate was a single continuous layer. This problem is the only low hypervelocity analysis that incorporated a cylindrical projectile.

7. ANALYTICAL RESULTS

Initial results, from the first four configurations, indicated that the interaction of the projectile with the front plate at 2.5 km/s had changed considerably from the previous impacts at 7 km/s. Very little projectile breakup was seen in any of the four cases. An example of these results is shown in Figure 31, a plot of the projectile and front plate material densities at 10 μsec after impact for problem 3.52. The projectile has completely penetrated the front plate and is still essentially intact. There is also a "cap" of high density front plate material on the leading edge of the projectile material. Problems 2.52 and 3.52, as mentioned earlier, only differed in the properties used for the aluminum projectile. Problem 3.52 used lower, more realistic values, of ultimate stress and strain. Comparison of the projectile breakup in the two cases at 4 μsec (Figure 32) shows that the properties change is important in the initial breakup, as the projectile of problem 3.52 is more broken up than the higher strength projectile of problem 2.52. This effect is still present at 15 μsec (Figure 33) after impact. However, the overall projectile breakup is still rather poor, even with the lower projectile strength, as can be seen in both Figures 32 and 33.

After initial analyses indicated changes in the front plate would be necessary to obtain projectile breakup, different front plate configurations were studied. Materials for study were selected on the bases of improved strength and volume density. Front plates of comparable areal densities but different materials were analyzed, including ceramic, stainless steel, and tungsten. As can be seen from Figure 33, the stainless steel front plate of problem 3.52 did not completely break up the projectile, an aluminum sphere. Similarly, tungsten and ceramic front plates were also ineffective. These results, specifically for problems 6.52 and 4.52, are shown in Figure 34. While some breakup has occurred, the large amount of contiguous high density material indicates the front plates are still inadequate to ensure shield success. An increase in ceramic thickness and,

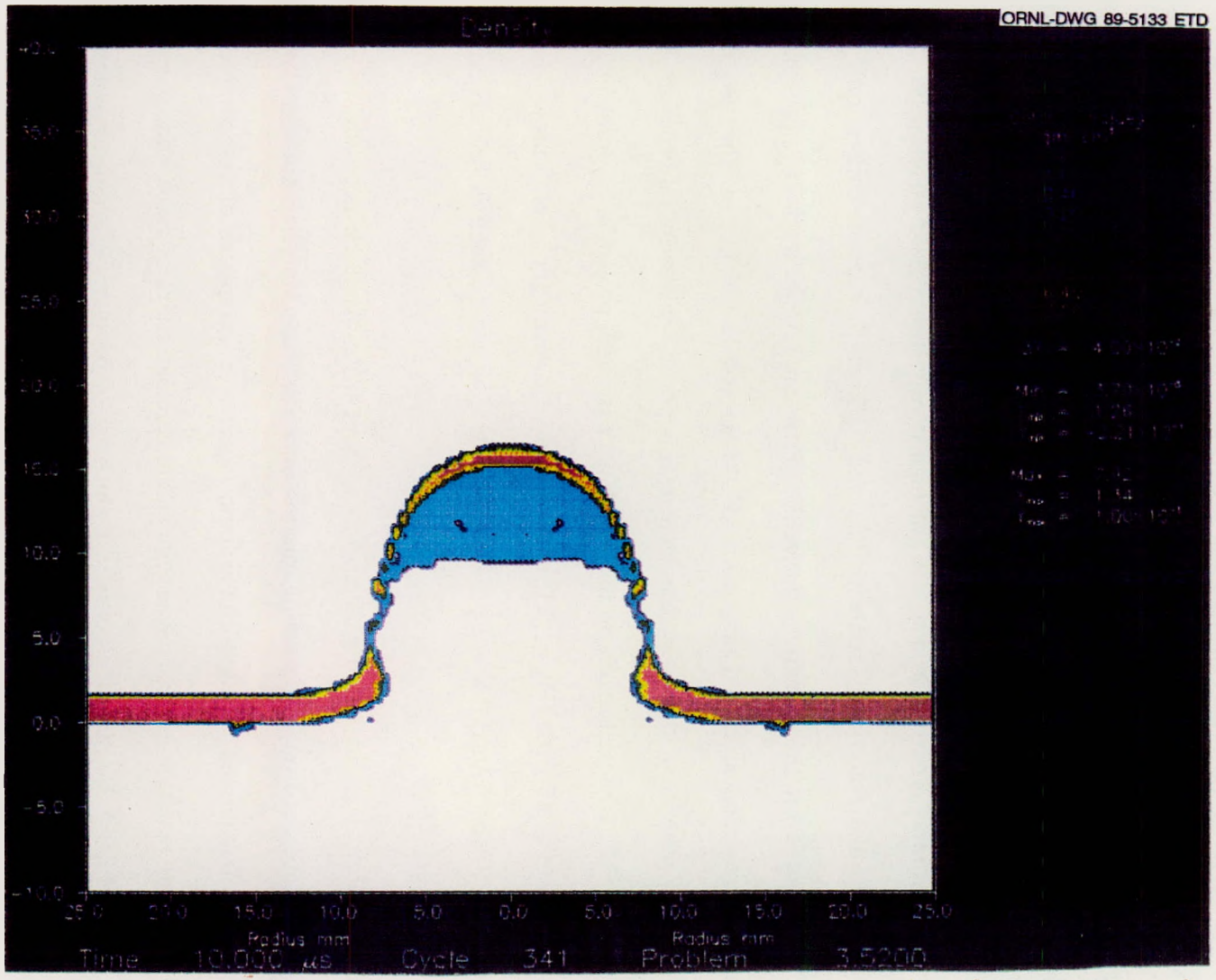

Figure 31. Problem 3.52 at 10 μsec

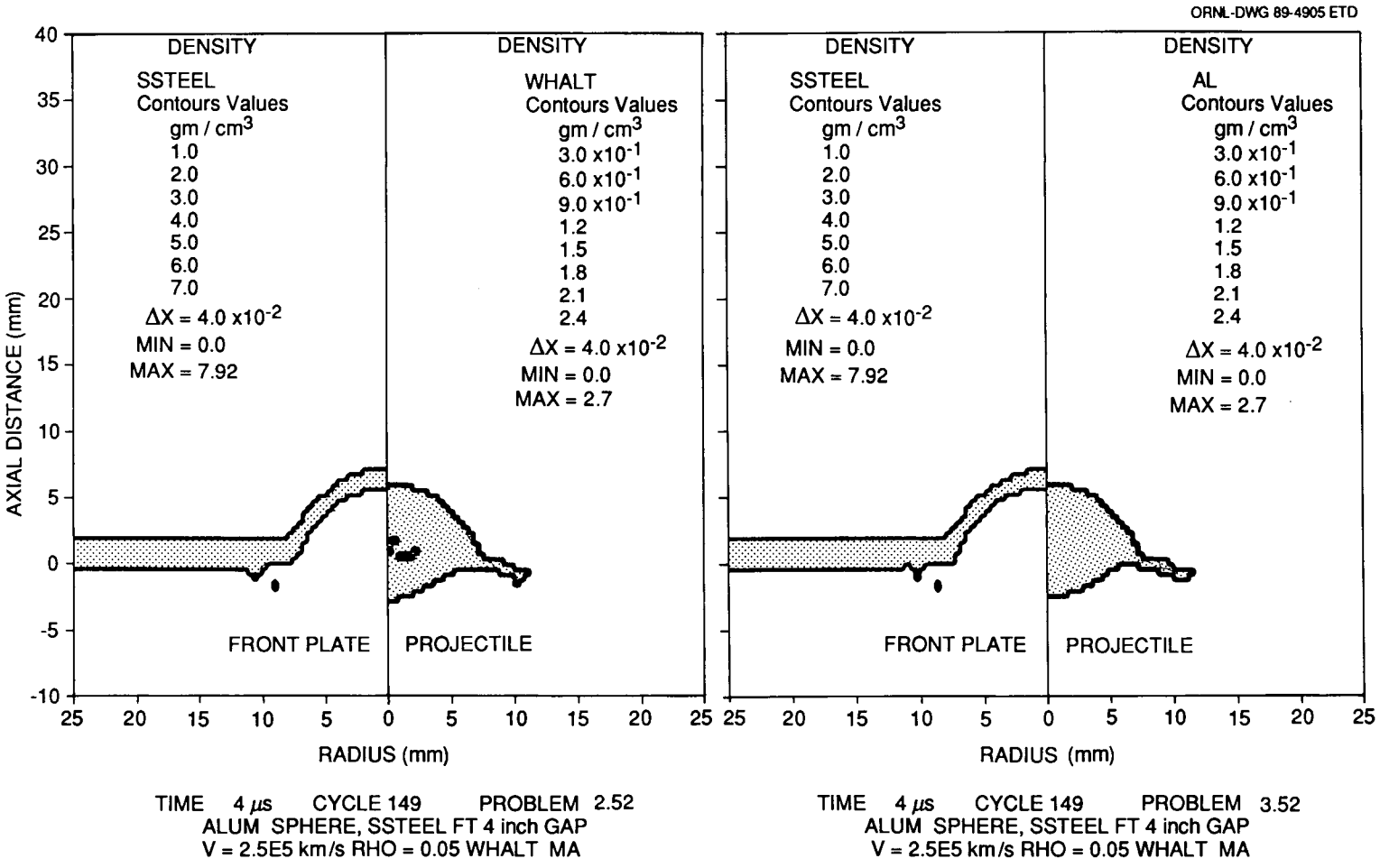

Figure 32. Comparison of problems 2.52 and 3.52 at 4 μsec

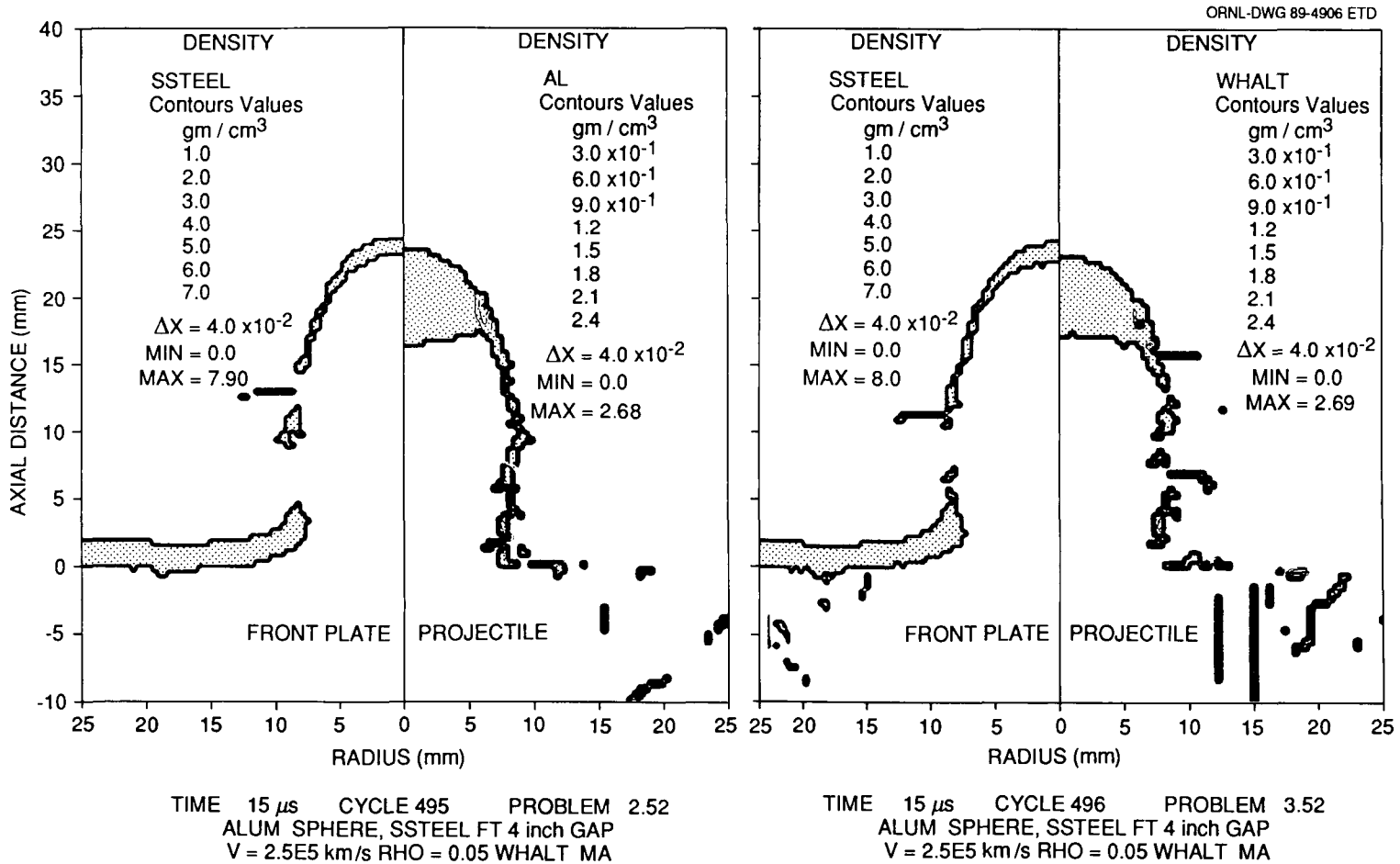

Figure 33. Comparison of problems 2.52 and 3.52 at 15 μsec

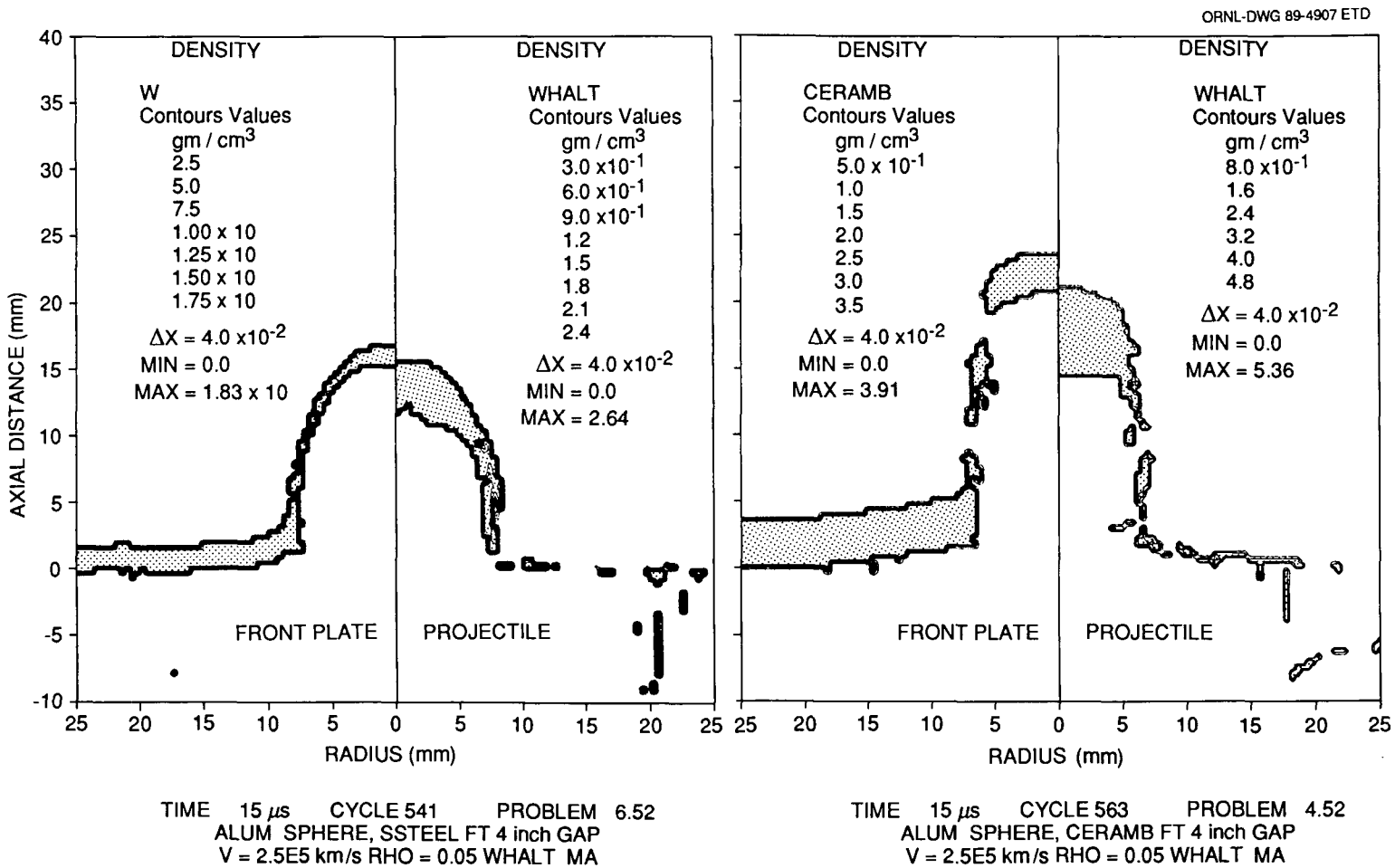

Figure 34. Comparison of problems 6.52 and 4.52 at 15 μsec

thus, areal density still did not provide adequate breakup, from the summary of results in Table 4 for problems 4.52 and 4.52(rev).

Velocity effects were analyzed also. Problems 5.52 and 4.52(rev) were identical in configuration with a velocity change the only difference. As listed in Table 4, at the projectile impact velocity of 2.5 km/s, projectile breakup was poor. However, an impact velocity change to 4 km/s resulted in excellent projectile breakup. This correlates well with the damage curve discussed earlier and shown in Figure 17. To better define the velocity effect, the configuration of problem 4.52 was analyzed again at impact velocities of 3.0 km/s (problem 7.52), 3.25 km/s (problem 3.42), and 4.0 km/s (problem 4.42). Projectile breakup was poor from 2.5 km/s through 3.25 km/s but again changed to excellent at the 4.0 km/s impact velocity. Thus the threshold of breakup lies between 3.25 and 4.0 km/s, again correlating well with the damage curve of Figure 17. Comparing Problem 5.52 and problem 4.52, shield and projectile materials are identical,, with the front plate of 5.52 twice the thickness of that of 4.52. The impact velocity of both problems was 4.0 km/s. The similarity in the excellent breakup of the projectile in both problems, even with the doubled areal density of one, indicates that material properties such as strength are of more importance than the areal density in this velocity regime.

Analytical work included a short study of two closely spaced ceramic front plates to determine if shock wave reinforcement could be achieved and, thus, provide projectile breakup. Three cases were studied; Figure 35 shows the results for these cases at 15 μsec. As can be seen in this figure, the projectile did not break up for any of the three configurations run. However, two advantages were seen in the dual front plate configuration. First, the velocity of the projectile was reduced by about 25% from the single plate configuration (Table 4). Also, the amount of front plate debris

ORNL-DWG 89-5134 ETD

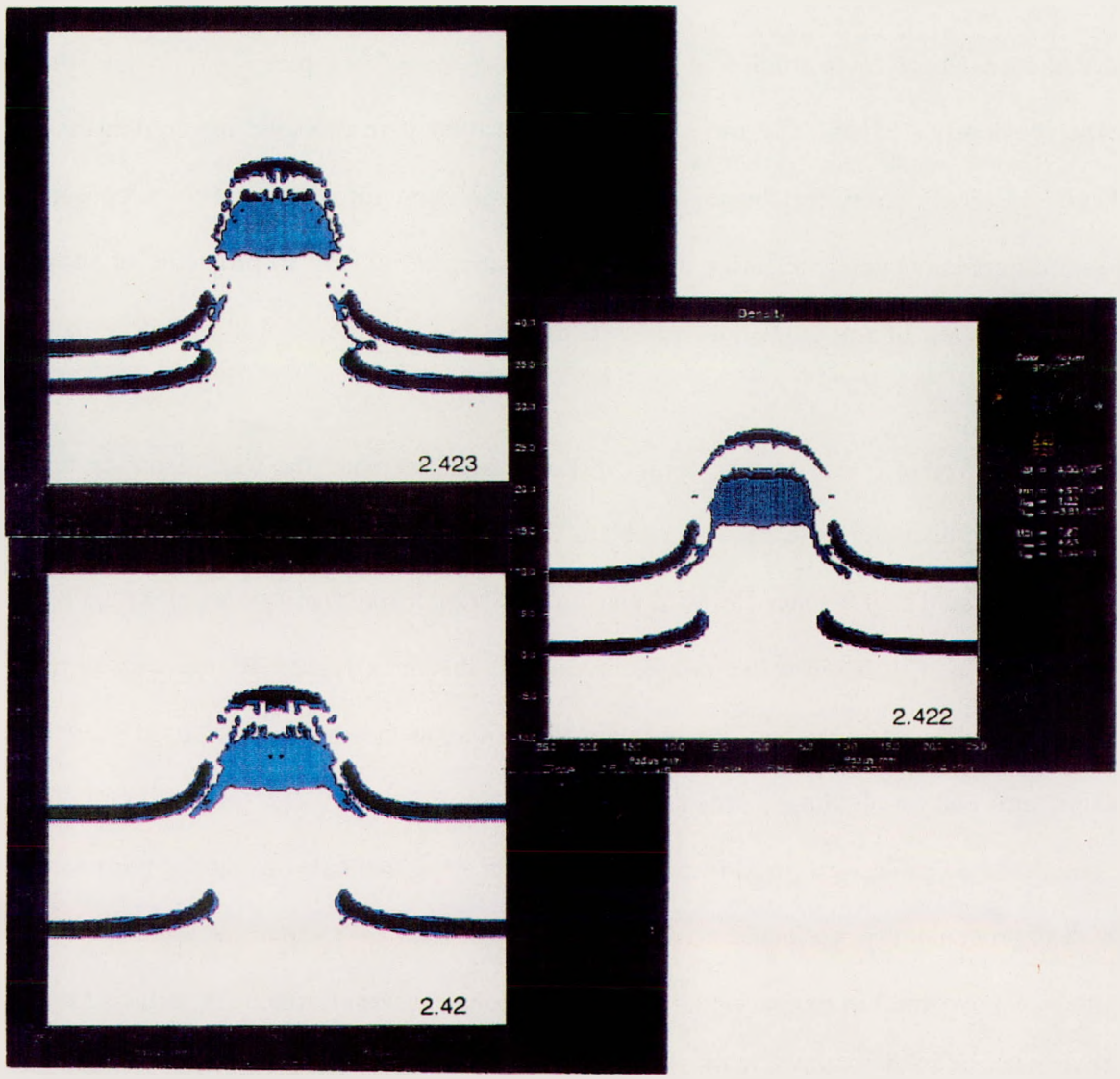

Figure 35. Results at 15 μsec for the spaced ceramic front plates

ahead of the projectile was less for these configurations than for the single ceramic plate configuration. This can be seen by comparison of Figures 35 with Figure 34, which shows the results of problem 4.52 (the single ceramic plate.)

Three of the analytical cases studied involved the use of wire front plates rather than the solid layer type previously studied. The use of a wire mesh rather than the solid material layers results in a decreased areal density for the same thickness. The diameter of the wire was chosen to be 1/4 of the projectile diameter, resulting in an areal density ratio of wire to projectile of about 0.20, whereas a solid plate of the same thickness would have an areal density ratio of close to 0.50.

A wide spacing (a wire center to wire center distance equal to twice the wire diameter, leaving a space of one wire diameter) was used in problem 9.112, and narrow spacing (a wire center to wire center distance equal to 1.5 times the wire diameter, leaving a space of one wire radius) was used in problems 9.15 and 9.16. The two configurations are shown in Figure 36, the density plots for problem 9.112 (wide spacing) and for problem 9.16 (narrow spacing) at 0.4 μsec after impact. Aluminum wire and an aluminum projectile were used in problems 9.112 and 9.16; tantalum wire and a tantalum projectile were used in problem 9.15. For the two cases using the narrow spacing, a marked improvement in projectile breakup over solid shields of comparable areal density ratios was noted. After careful investigation of the compressional wave patterns formed during the initial contact of the spherical projectile with the wires, it was seen that the pressure near the center of the projectile was enhanced by the delay in contact with the two outer wires. This pressure enhancement caused a much stronger tensile wave reflection from the back surface of the sphere and, thus, enhanced the projectile breakup. In the widely spaced configuration, this phenomena did not occur. Results for the two aluminum configurations at the wide and narrow spacings are shown in Figure 37. The large, centralized area of high pressure at 1.6 μsec is a good indicator

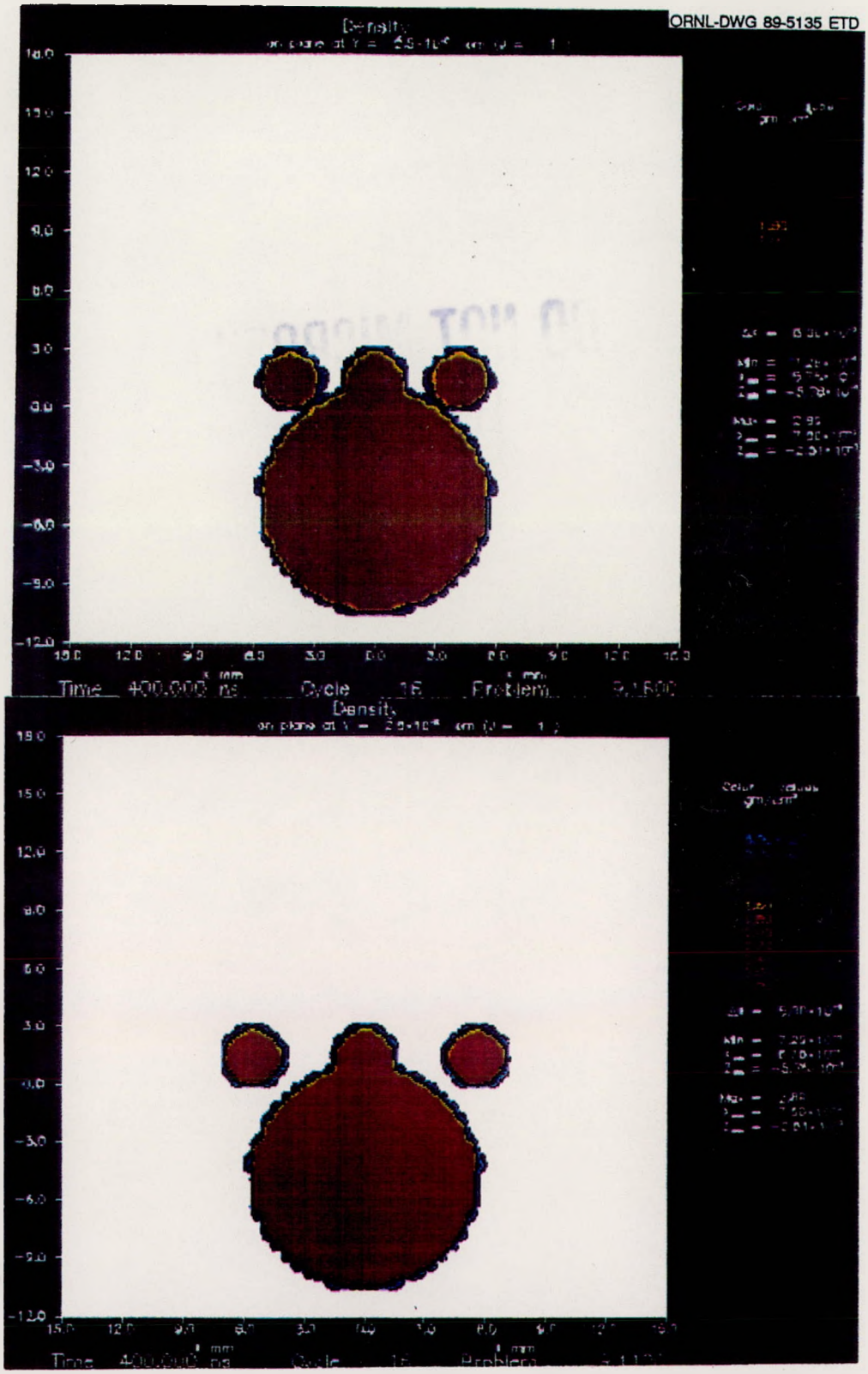

Figure 36. Density plots for problem 9.112 and 9.16 at 0.4 μsec

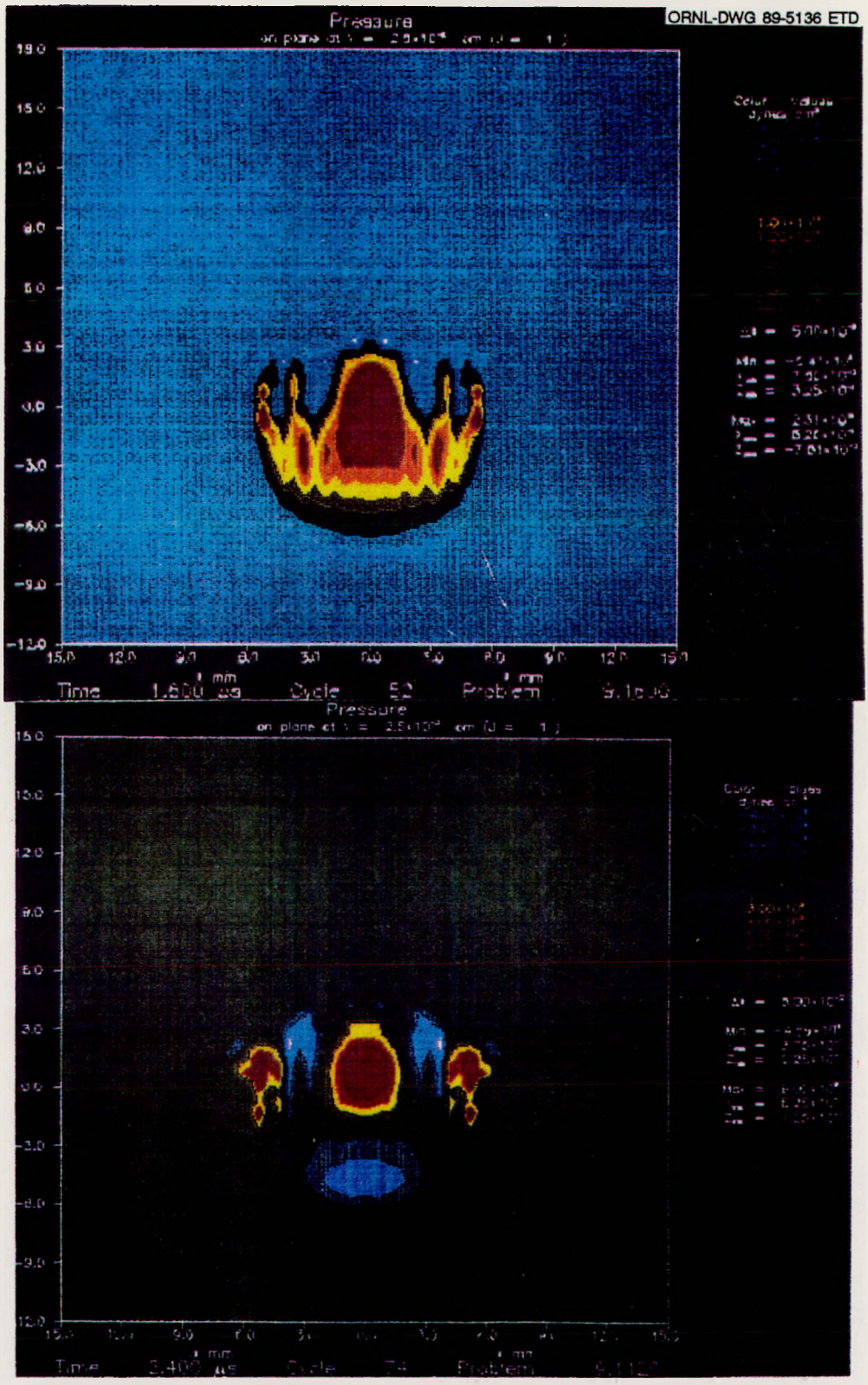

Figure 37. Pressure plots for problem 9.112 at 2.4 μsec and problem 9.16 at 1.6 μsec

of the ensuing projectile breakup for problem 9.16. In contrast, for problem 9.112 at 2.4 μsec, three separate and smaller high pressure areas are visible. Projectile breakup was poor for this configuration. The results for problem 3.15, the tantalum projectile into the closely spaced tantalum wire, were very similar to those of problem 9.16. It is significant to note that these results were for a spherical projectile. With the projectile breakup dependent upon the compression wave interaction set up by the initial contact phenomena, it is logical to predict that the breakup of a cylindrical projectile would require a differently configured front shield.

The A/B front plate configuration of shield 73 was modeled in problem 7.32. All parameters were set up to match the actual test configuration as nearly as possible. In shield 73, the A layer was composed of four thin layers, while for problem 7.32 the A layer was modeled by a single homogeneous layer of the same total thickness. Figure 38 is a density plot of this problem at 45 μsec after impact, containing the projectile, A layer, B layer, and disrupter materials. Points of interest in this plot include:

1. the compression wave in the disrupter just ahead of the A layer debris,
2. the large amount of material traveling into the shield,
3. shock waves in the A layer of ceramic,
4. the beginning of separation of the A and B layers with the aluminum B layer bending back into the disrupter, and
5. the length of time for complete front plate penetration.

Figure 39 shows the same problem at the same time, but the components are separated onto separate plots. From these plots, further notes of interest are the large amount of ceramic traveling into the shield and the good breakup of the projectile. While not visible from a density plot, the velocity reduction across the front plate was also significant, down to 0.68 km/s.

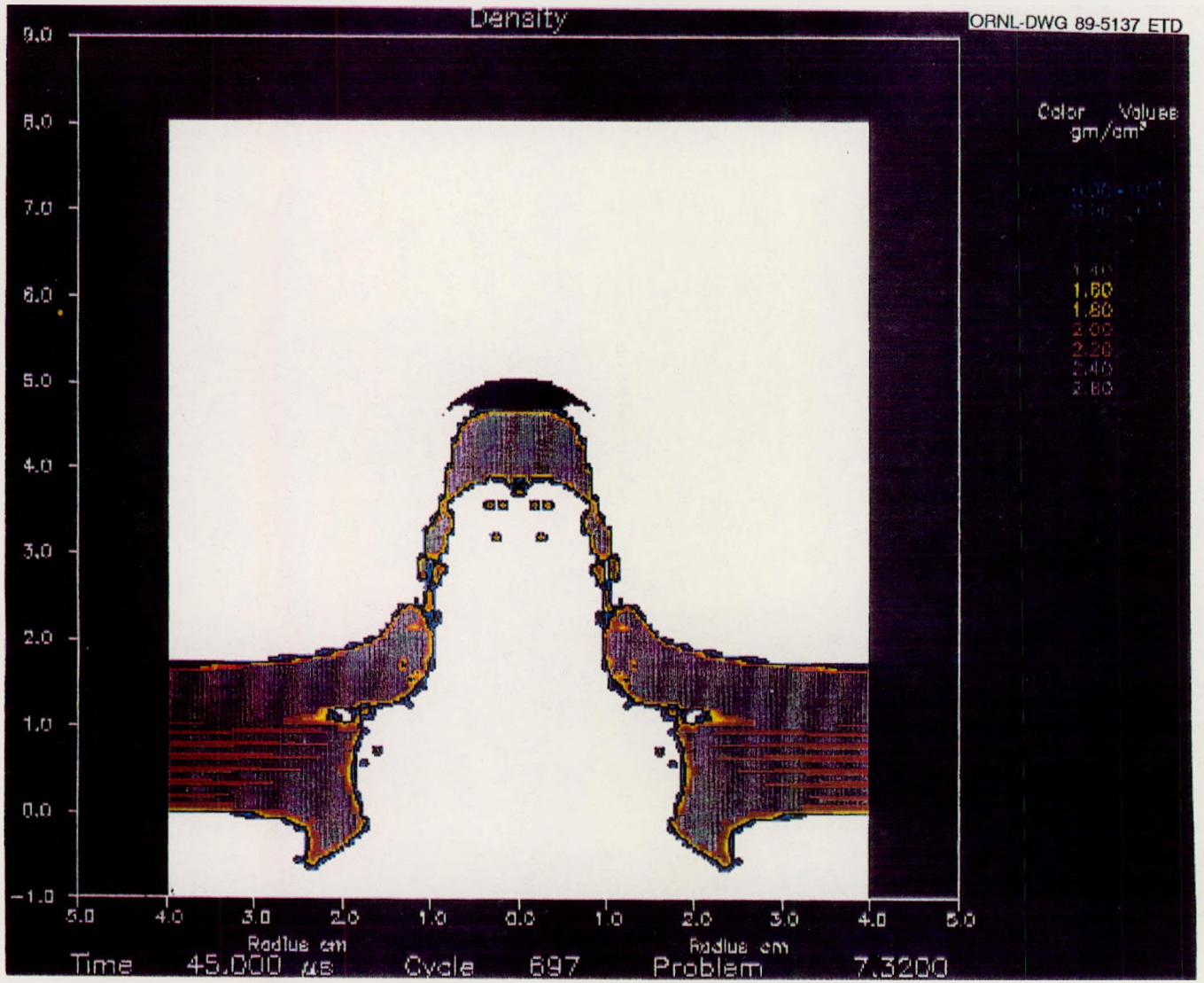

Figure 38. Problem 7.32 density plot at 45 μsec

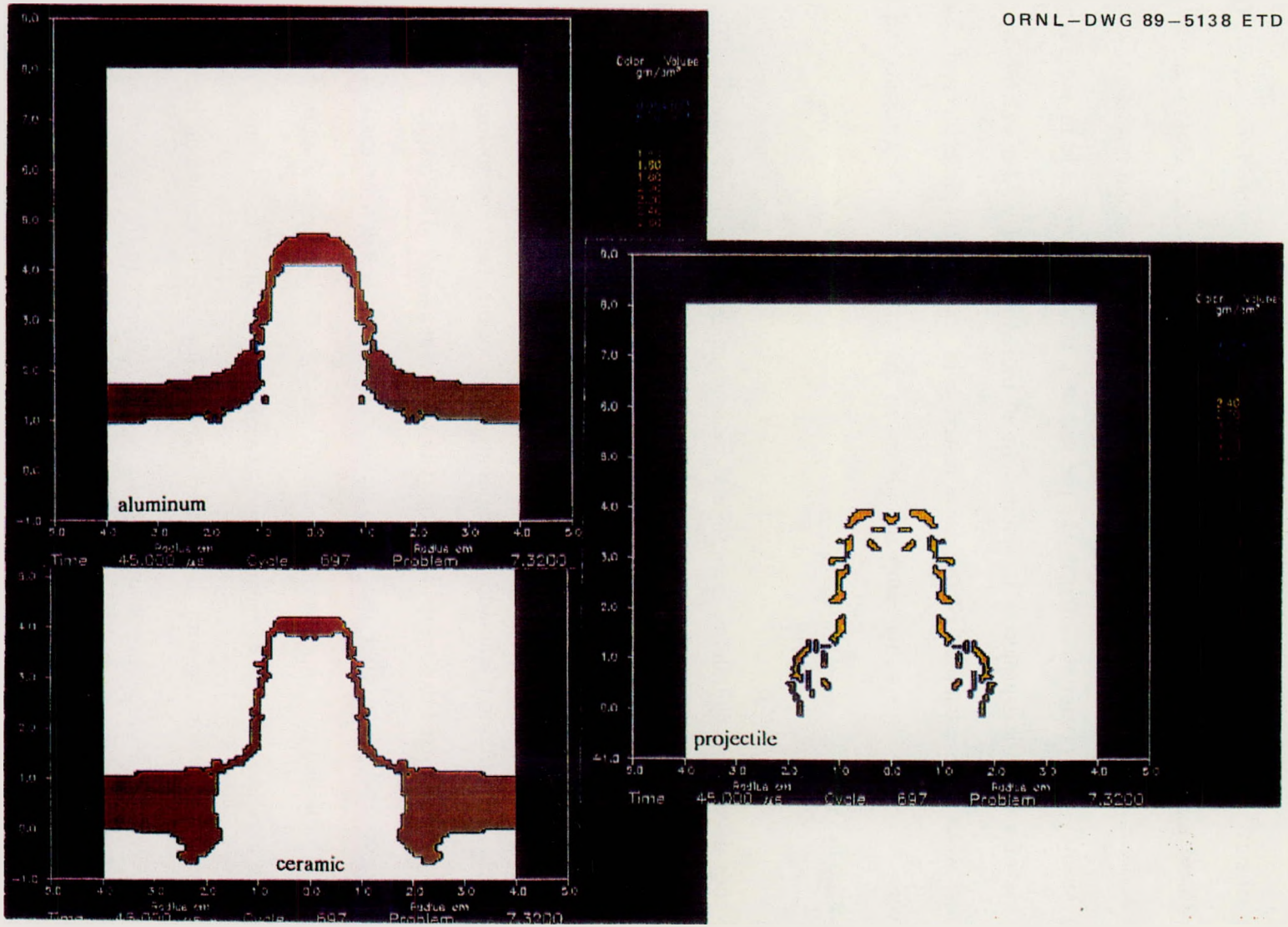

Figure 39. Individual component density plots for problem 7.32 at 45 μsec

8. COMPARISON OF ANALYTICAL AND TEST RESULTS

From the analytical results, the wire front shield looked to be a likely candidate for success. The wire front shield tested as shield 78, as previously discussed, was a failure. However, several differences between the analysis configuration and the test configuration could have significantly altered the results. The primary difference was the use of a spherical projectile in the analysis versus the use of a cylindrical projectile in testing. In all the analyses of wire front shields, the projectile and wires were composed of the same material; in test 78 the projectile and shield materials were different. No specific comparison between the analytical and test results can be made at this point.

Several of the analysis configurations incorporated ceramic materials as front shields. These analyses (problems 2.50 through 9.16 in Table 4) were all done prior to the testing of any ceramic materials. After test series 6, an attempt was made to model shield 73. These results are covered in Section 6. In comparing these results to the test results, the behavior of the B layer as modeled corresponds well. The dishing phenomena is beginning to be visible, referring to Figure 39, with the smooth entry and tapered exit lip shown also. The large aluminum cap corresponds well with the large piece of spall found after the test. Penetration took much longer for this analysis, agreeing well with the extremely long travel time during testing. The velocity reduction across the front plate was also large (Table 4), again agreeing well with the long travel time. Projectile breakup was good, corresponding with the shield success. However, in examining the modeled behavior of the ceramic material, important differences can be seen. In the analysis, the ceramic has not fractured and there is very little ejecta. A large amount of ceramic debris is shown traveling into the shield, referring to Figure 39. This is very different from the test results, as previously described.

Closer examination of the Hull code model for a ceramic material was performed. Several small problems were set up and run for short times to analyze the effect of material property changes on material behavior for a brittle material. None of the changes made resulted in a brittle fracture upon impact, as seen during testing. Work was underway to resolve this problem at the time of program termination.

9. CONCLUSIONS AND RECOMMENDATIONS

Due to the limited data obtained, at this point the conclusions made are primarily indications of areas for further work.

1. The 3 km/s threat is potentially quite damaging, especially in comparison with the same projectile at 7 km/s. Weight reduction for a layered shield versus the solid homogeneous aluminum shield is more difficult for the 3 km/s threat than the 7 km/s threat. Two phenomena combine to cause this difficulty: (1) the high damage at 3 km/s for layered shields due to a lack of good projectile breakup and (2) the lower weight of the solid aluminum reference shield for weight reduction measurement. Shield design is made more difficult by the projectile breakup mode, which inherently limits the effectiveness of the layered shield concept. However, the projectile energy rather than the projectile breakup is the governing factor for the solid shields, leading to a lower reference shield for comparison. These points are well illustrated by comparison of the shield weights for the same aluminum projectile at the two velocities, both for the solid aluminum reference shields and for the lightest weight successful layered shields. The most important of these comparisons is the weight reduction seen for shield 79/81, the configuration successful against both velocities. The same configuration is a weight reduction down to 16.7% of the reference solid shield for the 7 km/s test, but only 41.5% of the reference weight for the 3 km/s test. While this shield, designed for the 3 km/s threat, was also successful against the 7 km/s threat, the results of this study indicate that a broad generalization along these lines cannot be made. The variation in front plate configuration for a successful 3 km/s shield is very important and may override the projectile breakup phenomenon seen at 7 km/s. Analysis of the reverse situation, a 7 km/s

shield tested at 3 km/s, indicates that the high velocity shield would be very likely to fail at the lower impact velocity.

2. The front shield is very important in the overall shield performance; wire front shields and the A/B type front shields need further study. In the A/B type front shield, the solid aluminum B shield specifically is a very likely candidate for weight reduction by a material change. Single-layer homogenous metal front plates do not appear to be a good choice either for performance or for weight reduction. Further analysis and/or testing in the area of spaced layered front shields would be of interest; the limited amount of study to date does not clearly show a significant performance improvement, but the data are very limited.

3. The analysis of ceramic (brittle) materials should be continued with an effort devoted to obtaining an accurate hydrocode model for this type material.

4. Experimental work using ceramic materials should be continued also. Sublayering, confinement, bonding to the backup plate, how the ceramic and projectile interact, and debris/ejecta produced are all areas of interest.

5. In the low hypervelocity region, a transition from ballistic impact phenomena which are dependent upon properties such as strength and hardness, to the hypervelocity impact phenomena which depend on material densities, change of state energies, etc., is underway. The low hypervelocity region impact phenomena appear to be affected by a range of material properties. Widely different impact phenomena, from dishing (affected by material strength and observed at low velocities) to the formation of an axisymmetric hole (characteristic of high

velocity impact and high energy deposition), can be seen in the different shields, all initially impacted at 3 km/s. Material property effects need to be better defined and characterized.

6. Overall, a significant weight reduction was achieved. Further weight reduction could be obtained. Additional study of the function and desired characteristics of all the shield layers is recommended.

10. REFERENCES

Brewer, E. D., "Shield Testing Against Ballistic Projectiles," in press, ORNL-TM , prepared under U.S. DOE Contract DE-ACO5-84OR21400.

Brewer, E. D., "Spaced Array Shield Design, Analysis, and Testing To Survive Stainless Steel Projectiles," in press, ORNL-TM , prepared under U.S. DOE Contract DE-AC05-84OR21400.

Goldsmith, W. and Finnegan, S. A., "Penetration and Perforation Processes in Metal Targets at and Above Ballistics Velocities," International Journal of Mechanical Science, Vol 13, pp. 843-866, 1971.

Hopkins, S. K., Lee, T. W., and Swift, H. F., J. Spacecraft 9, 1972.

Mah, R. and Martell, P., "ATAC and the Armor/Anti-Armor Program," Los Alamos Science, pp. 51-63, Summer 1989.

Matuska, D. A. and Osborn, J. I., "Hull Hydrocode Documentation, User's Manual," 1983, revised October, 1987, Orlando Technology, Inc., Shaliman, Florida.

Nicol, B., Pattie, S. D., O'Donnell, R. G., and Woodward, R. L., "Fracture of Ceramics in Composite Armours," Fracture Mechanics in Engineering Practice Conference Proceedings, pp. 150-156, November 1988.

ORNL Staff, "Final Report of the Technical Progress on the Oak Ridge Fast Track Program April 1986 - September 1987 (U)," March 1989, prepared under U.S. DOE Contract DE-ACO5-84OR21400.

Piekutowski, A. J., "Debris Clouds Generated by Hypervelocity Impact of Cylindrical Projectiles with Thin Aluminum Plates," International Journal of Impact Engineering, Vol. 5, pp. 509-518, 1987.

Sandstrom, D. J., "Armor/Anti-Armor Materials by Design," Los Alamos Science, pp. 36-50, Summer 1989.

Smith, J.E., "Experimental Methods, "ORNL-TM , in press.

Thomas, D. G., Brewer, E. D., Hendrich, W. R., and Smith, J. E., "Front Plate and Projectile Variance Results," ORNL-TM , in press.

Thomson, W. T., "An Approximate Theory of Armor Penetration," Journal of Applied Physics, Vol 26 No.1, pp. 80-82, January 1955.

Wilkins, M. L., Cline, C. F., and Hondel, C. A., "Light Armor," UCRL-71817 Preprint, Lawrence Livermore National Laboratory, July 1969.